TWO DEGREES OF FREEDOM VARIABLE STRUCTURE MECHANISMS DESIGN

A THESIS SUBMITTED TO

THE GRADUATE SCHOOL OF NATURAL AND APPLIED SCIENCES

OF

THE MIDDLE EAST TECHNICAL UNIVERSITY

BY

ENGİN TANIK

IN PARTIAL FULFILLMENT OF THE REQUIREMENTS FOR THE DEGREE

OF MASTER OF SCIENCE

IN

THE DEPARTMENT OF MECHANICAL ENGINEERING

SEPTEMBER 2001

Approval of the Graduate School of the Middle East Technical University

Prof. Dr. Tayfur ÖZTÜRK
Director

I certify that this thesis satisfies all the requirements as a thesis for the degree of Master of Science.

Prof. Dr. Eres SÖYLEMEZ
Head of Department

This is to certify that we have read this thesis and that in our opinion it is fully adequate, in scope and quality, as a thesis for the degree of Master of Science.

Prof. Dr. Eres SÖYLEMEZ
Supervisor

Examining Committee Members

Prof. Dr. S. Turgut TÜMER

Prof. Dr. Eres SÖYLEMEZ

Prof. Dr. Kemal İDER

Assoc. Prof. Dr. Mehmet EROĞLU

Dr. Ergin TÖNÜK

ABSTRACT

TWO DEGREES OF FREEDOM VARIABLE STRUCTURE MECHANISMS DESIGN

TANIK, Engin

M.S, Department of Mechanical Engineering

Supervisor: Prof. Dr. Eres Söylemez

September 2001, 77 pages

The aim of this study is to introduce some flexibility to two degree-of-freedom closed-loop mechanisms. A synthesis procedure for two different types of seven-link mechanisms for different output oscillations is considered. One of the freedoms is used as a digital control for flexibility. Switching conditions are also investigated.

Key words: Variable Structure Mechanisms, Threshold Switch, Two Degrees of Freedom Seven-Link Mechanisms.

ÖZ

İKİ SERBESTLİK DERECELİ DEĞİŞKEN YAPILI MEKANİZMA TASARIMI

TANIK, Engin

Yüksek Lisans, Makina Mühendisliği Bölümü

Tez Yöneticisi: Prof. Dr. Eres Söylemez

Eylül 2001, 77 Sayfa

Bu çalışmanın amacı, iki serbestlik derecesine sahip olan kapalı devre mekanizmalarına esneslik kazandırmaktır. Bu doğrultuda ele alınan yedi-uzuvlu bir mekanizma için geliştirilmiş bir tasarım metodu anlatılmaktadır. Bir serbestlik derecesi esneklik için, dijital kontrol olarak kullanılmıştır. Bir konumdan diğer konuma geçiş şartları da incelenmiştir.

Anahtar Kelimeler: Değişken Yapılı Mekanizmalar, Eşik Anahtarı, İki Serbestlik Dereceli Yedi Uzuvlu Mekanizmalar.

To my parents...

ACKNOWLEDGMENTS

The author expresses sincere appreciation to Prof. Dr. Eres Söylemez for his guidance and insight throughout the research.

The author would also like to thank his mother (Semra Tanık) and his father (Prof. Dr. Yalçın Tanık) for their continuos support.

TABLE of CONTENTS

LIST of FIGURES

Figures:

CHAPTER 1

INTRODUCTION

Commonly used closed-loop mechanisms can work at high-speeds, require less maintenance and are inexpensive to manufacture. However, they are inherently inflexible. The aim of this study is to introduce some flexibility to closed-loop mechanisms with two degree-of-freedom structures by using one of the freedoms as a digital control.

A synthesis procedure for two different types of seven-link mechanisms is derived. These mechanisms run as six-link mechanisms for different positions of the control-link to achieve the required output oscillations. One of the mechanisms synthesized is analyzed in detail for low and high-speed operations considering the static and dynamic forces. Through this analysis, it is shown that both low and high-speed switching (the motion of the control-link to a pre-determined position to obtain different oscillation amplitude at the output-link) is possible when certain conditions are satisfied. During switching mechanism is also analyzed in order to prove that it is also movable.

CHAPTER 2

LITERATURE SURVEY

Robots are extremely handy for accommodating variations within a given task, but if these variations are limited in number, sometimes a less expensive, more efficient mechanism can accomplish the same task. Also, these multi-actuator designs are heavy, and slow in operation, and they demand sophisticated maintenance and occupy lots of floor space. It is not uncommon to see multi-axis robots performing simple tasks. Very rarely, these overly flexible and expensive robots are reprogrammed to perform many different tasks.

Sometimes, when small amount of flexibility is needed, closed-loop mechanisms with a limited flexibility are used. The primary advantages of closed-loop mechanisms are cost effectiveness, reliability, repeatability, low inertia, and high-speed capability. These mechanisms must be multi degree-of-freedom to provide flexibility but can be unconstrained (differential of the car, for instance) or constrained.

There are two different fields in the literature, which the current study, is related.

i. Multi Degree-of-Freedom Mechanisms

ii. Mechanical Logic Systems

2.1 Multi Degree-of-Freedom Mechanisms

Degree-of-freedom of mechanisms must be greater than one, to achieve flexibility. This part is related with recent study about kinematic synthesis methods of some multi degree-of-freedom mechanisms.

Mruthyunjaya [1] presented a graphical method for synthesis of the general, seven-link, two degree-of-freedom planar linkage (Figure 2.1) to generate functions of two variables. The method is based on point position reduction and permits synthesis of the linkage to satisfy up to six arbitrarily selected precision positions.

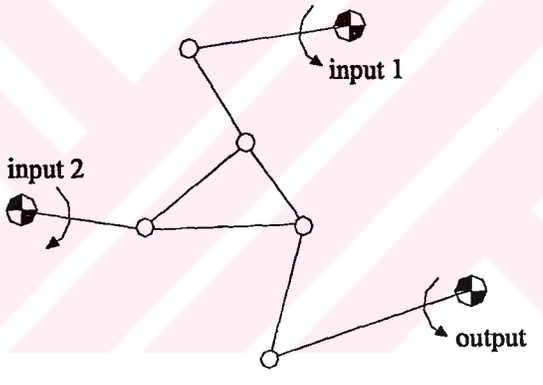

Figure 2.1: General Two Degree-of-Freedom Linkage

Handra-Luca [2] discussed the basic principles of six-bar linkages with adjustable output oscillations. One such mechanism is shown in Figure 2.2. This mechanism is made up of four-bar *ABCD* to which *CED* has been added. The input-link is *AB* and the output link is $\dot{E}G$. Displacing the fixed joint *D* to various positions causes a variation in the magnitude of the output-link's oscillation. At a given moment the joint *D* overlaps joint *E* at point *H* (*CD* must be equal to *CE* simultaneously), so the output-link remains at rest for a rotation of the crank.

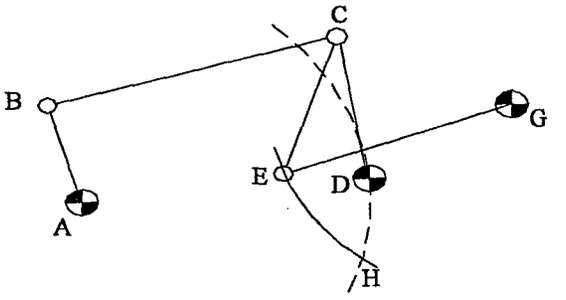

Figure 2.2: Adjustable Oscillation Six-link Mechanism

His other examples to adjustable oscillation mechanisms are shown in Figure 2.3.

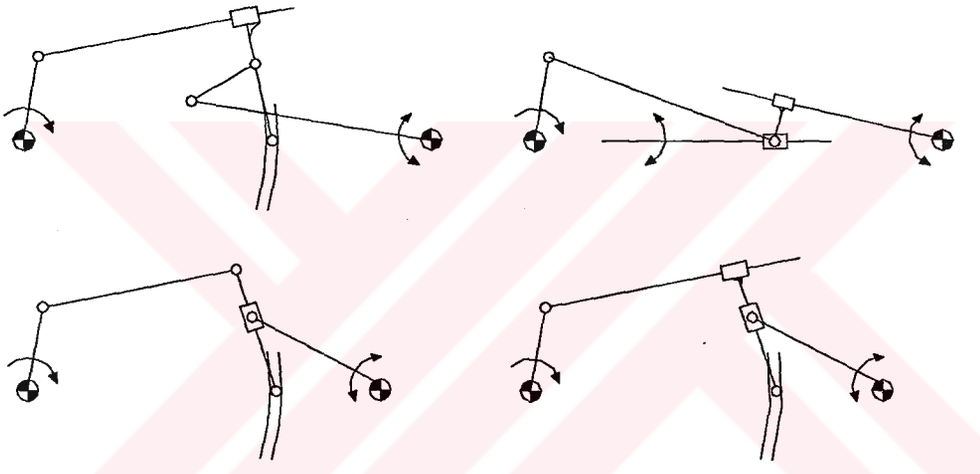

Figure 2.3: Adjustable Oscillation Six-Link Mechanisms

Kohli and Soni [3] found a synthesis technique to design for varieties of synthesis problems for seven-link mechanisms with two degrees of freedom. Their synthesis method involves the application of displacement matrices to derive synthesis equations. They considered the following types of synthesis problems:

1- Rigid body guidance as a function of two variables,

2- Rigid body guidance coordinated with point path,

3- Point-path generation coordinated with motions of one output and two input links,

4- Point-path generation,

5- Point-path generation as a function of two variables controlled by two inputs,

6- Function generation of two variables.

Synthesis equations of problems (1), (2) and (3) are solved in closed-form and the non-linear synthesis equations of problems (4), (5) and (6) are solved numerically.

Ahmad and Waldron [4] considered synthesis techniques for 4-bar linkages, having adjustable driven crank pivots, for different motion generation problems.

Chuenchom and Kota [5] discussed analytical methods for designing adjustable mechanisms based on synthesis of adjustable dyads. They developed a generalized synthesis method to design such mechanisms that can perform multiple tasks through programmed adjustment of one or more of the link parameters. In a five precision-point, adjustable dyad synthesis for four different types of adjustments is made by:

1-) the length of the input vector

2-) the length of the ground pivot

3-) the angle of the ground-pivot vector

4-) the length of a coupler vector.

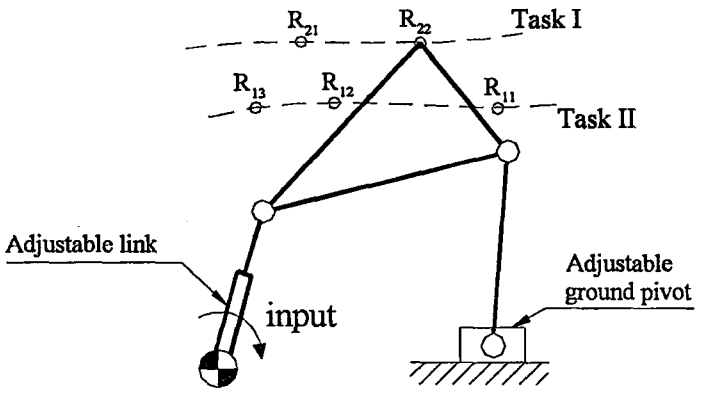

Figure 2.4: Adjustable Four-Bar Linkage

As an example, an adjustable four-bar linkage with two adjustable parameters is shown in Figure 2.4, in two different positions corresponding to two different motion-generation tasks.

A. Akmeşe and E. Söylemez [6] synthesized serially connected two four-bar mechanisms, that performs variable output-link oscillation. (Figure 2.5). By changing the position of the control-link *AD*, which is the fixed link of the second four-bar, the output-link oscillation changes. Since the control-link is the fixed link of the first four-bar mechanism, the proportions of the first four bar mechanism doesn't change. A. Akmeşe also analyzed the mechansim for switching the control-link from one position to other, due the torque variation at the output-link.

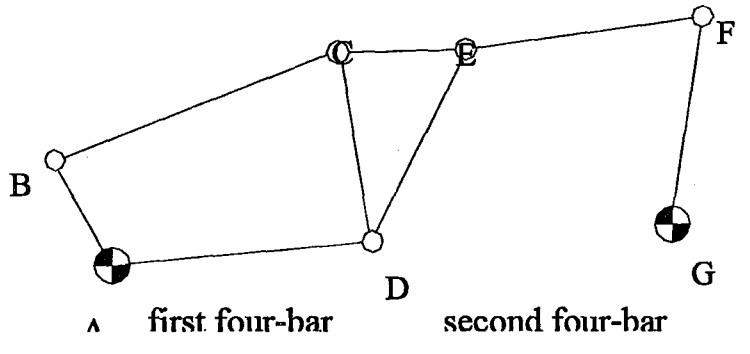

Figure 2.5: Serially connected two Four-Bar Mechanisms

Kireçci, Dülger and Gültekin [7] used a seven-link, two degree-of-freedom mechanism, (Figure 2.6) for variable oscillation at output. The input to the

mechanism is at link 2 and the translational adjustment at link 5 provides variable oscillation. However, since the adjustment control system is mounted on link 4, which is driven by a servomotor, the inertia of link 4 increases. So, at high-speed operations the forces become larger.

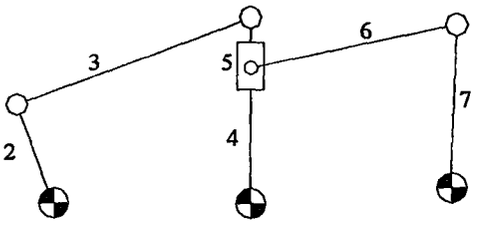

Figure 2.6: Variable Oscillation Mechanism with Translational Adjustment

2.2 Logic Systems

In multi degree-of-freedom closed-loop mechanisms, the number of the inputs may be equal (constrained) or less (unconstrained) than the degree-of-freedom of the mechanism. In other words, if the mechanism is constrained, every independent input is controlled externally by an actuator. For unconstrained mechanisms, the motion is constrained by the external forces and dynamic characteristics of the system (i.e. differential of a car). So cost and complexity of the system decreases, if it is unconstrained.

After the kinematic synthesis of the mechanism, switching analysis will be done to investigate to control one of the degrees of freedom of the mechanisms, by means of torque variation at the output. Also, there must be a logic system attached to the control-link, in order to switch from one position to other due to torque variation.

A very simple, mechanical logic system used in some press machines that are shown in Figure 2.7. The control system is placed on the coupler-link of the four-bar mechanism. (Despite the mechanism has five links, it can be called as four bar since, normally, there is no relative motion between link 3 and 4). If there is an

unexpected torque increase on the output-link (5) which also causes compression force increase on link 4, the pre-load on the slider (by the spring force on the ball) will be exceeded. So, the slider won't remain stationary and the force transmission will stop. This control system can be called as mechanical fuse, which eliminates a complex and expensive brake system.

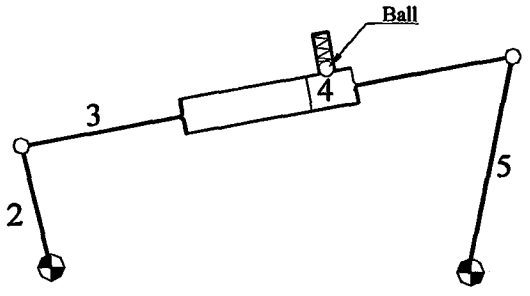

Figure 2.7: Crank-Rocker of a Press

A mechanical logic system, that can be adapted to the control-link *(AD)* of a two degree-of-freedom seven-link mechanism in Figure 2.5, is shown in Figure 2.8. This system forces the control link to be stable in two positions according to the torque variation on this link. If a counter clockwise torque larger than the threshold value is applied to the control link, similar to the press switch, the link releases from the first groove and moves to the second one. After the force analysis of the mechanism, the torque applied to the control-link can be found and the threshold values of the logic system in two positions can be determined according to desired switching timing, if possible.

Depth of the grooves on the fixed link determines the threshold torque values of the switch. Adjustment screw, which is on the control-link, can not directly control the threshold values in two positions. Because, if the pre-load of the spring is changed by the setscrew the threshold values will increase or decrease for two positions simultaneously, which is not desired.

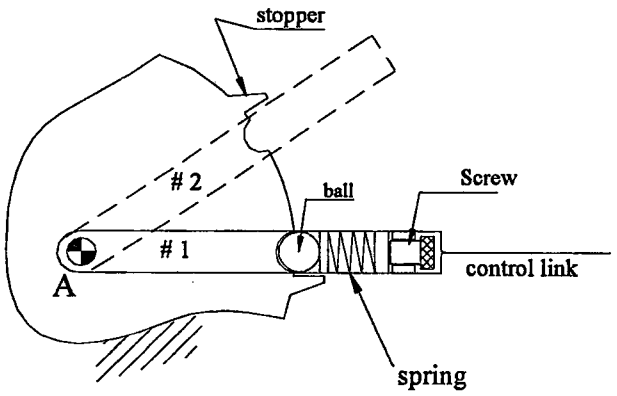

Figure 2.8: A Typical Switch Element

As an alternative, the positions of the switch elements can be changed. The setscrew, spring and the ball will be on the fixed-link and a grooved section can be processed on the control-link. Therefore, with screws on the fixed-link, the threshold values can easily be determined by trial and error, when the mechanism is working as well. In addition, the mass moment of inertia of the control-link decreases. The only disadvantage of this layout is the increase in the cost.

A mechanical logic element, multi-port lever, investigated by Söylemez and Freudenstein [8] is shown in Figure 2.9. This is a multi degree-of-freedom multi-port-lever configuration involves a link, the plane displacement of which is a rotation about one of several parallel axes or ports. Connecting rods connect the ports to sliders on both sides of each port and the sliders are loaded by compression springs. At point O the lever is actuated by an initially horizontal force, P, called control force.

If the magnitude of the control force increases slowly from zero, a force level will be reached at which the lever will just begin to move. The motion of the lever will be rotation about one of the ports, which is a function the force exerted by the springs.

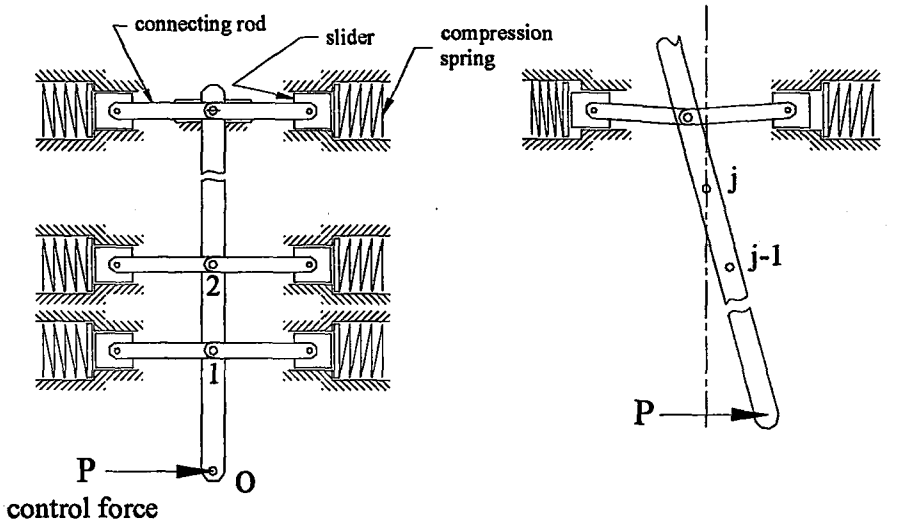

Figure 2.9: Multiport Lever

Strap tool is an application of two-port lever, which tightens and automatically cuts off a plastic strap about a bundle of wires.

CHAPTER 3

KINEMATIC SYNTHESIS of TWO DEGREES of FREEDOM SEVEN-LINK MECHANISMS

3.1 Introduction

In this study, two different types of seven-link two degree-of-freedom mechanisms are taken into consideration, to explain a kinematic synthesis technique that is derived.

The first type of variable structure mechanism, shown in Figure 3.1, is formed by two slider-crank mechanisms that are connected serially with a common slider. The first slider-crank is an in-line type and the second one has an eccentricity. A full rotary input to the mechanism is at link b_2, and link a_2 is the output. The second input to the mechanism is at link b_1, called control-link, which is also the fixed link of the first slider-crank. Different positions of this link changes the eccentricity of the second slider-crank, while the link proportions of the first slider crank therefore the stroke remains the same.

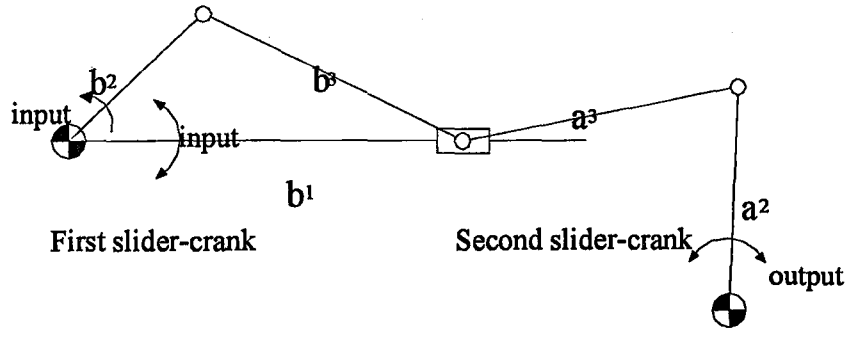

Figure 3.1: Seven-Link Variable Oscillation Mechanism

So, for different eccentricity with the same stroke, variable output-link oscillations can be obtained.

The second type of variable structure mechanism, in Figure 3.2, is composed of a four-bar and a slider-crank mechanism that are serially connected. This mechanism can be called as "Variable Stroke Mechanism". A full rotary input is at link b_2, therefore the four-bar must be crank-rocker type and the output link a_4 makes translatory oscillations. Second input to the mechanism is at link b_1, called control-link, which is also the fixed link of the four-bar. Similar to the first mechanism, different positions of this link changes the eccentricity of the slider-crank, while link proportions of the four-bar therefore the swing of link b_4 remains the same. Therefore, variation in eccentricity causes different output-link oscillations.

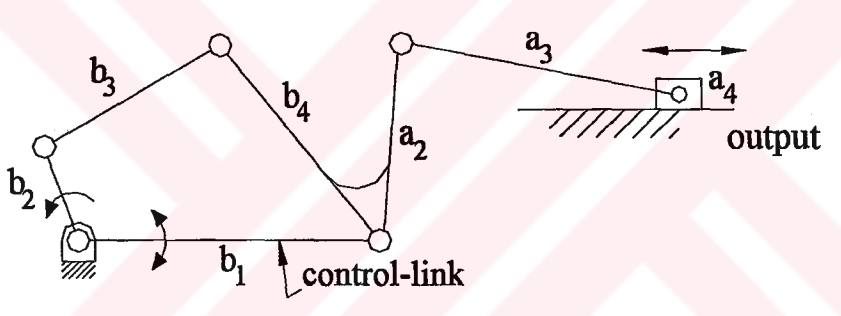

Figure 3.2: Seven-Link Variable Stroke Mechanism

After the kinematic synthesis of the mechanisms, optimization of the mechanisms will be done according to the following objectives:

- Reasonable link length proportions,
- Appropriate transmission angles to minimize the bearing loads and to avoid locking.

After force analysis, unless appropriate control-link torque characteristic is obtained to make switching possible, modifying the torque curve variations, as desired, will also be optimization objective.

3.2 Synthesis Procedure of the First Type of Seven-Link Mechanism

The synthesis of the seven-link mechanism (Figure 3.1) will be performed in two steps according to the required two different output-link swing. Initially, the second slider- crank will be designed for the larger swing angle. Then, the second axis of the slider will be determined to obtain the smaller swing angle with the same stroke. At the last step the first slider-crank mechanism, which is an in-line type will be synthesized according to known parameters.

Since this seven-link mechanism is composed of two serially connected slider-cranks, the transmission angle of each mechanism must be taken into consideration separately. The transmission angle of the first slider-crank mechanism is in between the normal line to slider axis and the connecting rod (b_3). Whereas, the transmission angle of the second slider-crank is in between links a_2 and a_3 since the input to the mechanism is at the slider and the output is at link a_2. Minimization of deviation of these transmission angles from 90^0 is required to prevent locking. In addition, transmission angle of the second slider-crank mechanism at second position must be checked, as the eccentricity and the output-link positions of the second slider-crank changes.

During the synthesis procedure, some subscripts are used for the output link angle and the slider position of the second slider-crank mechanism. Subscript "e" stands for extended position and "f" stands for folded position of the first slider-crank mechanism. Subscript "1" stands for the first position and "2" stands for the second position of the control-link where at first position the larger swing angle is obtained at the output link.

When the control-link of the mechanism is at its first position, this position will simply be called as "The first position of the mechanism". In second position of the control-link, the structure will be called as "The second position of the mechanism".

3.2.1 Formulation of the Seven-Link Mechanism

3.2.1.1 Determination of the Link Proportions According to the First Swing Angle

Initially second slider crank will be designed for arbitrarily selected initial slider position s_{e1} and corresponding output angle θ_{e1} according to larger swing angle.

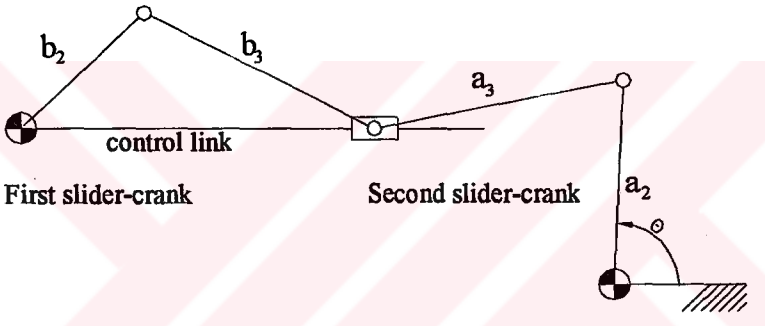

Figure 3.3: Seven-Link Variable Structure Mechanism

Freudenstein's equation, which is the relation between stroke and crank angle for the second slider-crank mechanism is:

$$s^2 = K1 \cdot s \cdot \cos\theta + K2 \cdot \sin\theta - K3$$

Where:

$$K1 = 2 \cdot a_2, \quad K2 = 2 \cdot a_2 \cdot c, \quad K3 = a_2^2 - a_3^2 + c^2.$$

According to the given initial slider position s_{e1} and output-link angle θ_{e1}, by taking the stroke Δs as unity, two equations for the required first swing angle $\Delta\theta_1$ are obtained.

When the first slider-crank is at extended position:

$$s_{e1}^{\ 2} = K1 \cdot s_{e1} \cdot \cos\theta_{e1} + K2 \cdot \sin\theta_{e1} - K3 . \qquad (3.1)$$

When the first slider-crank is at folded position:

$$s_{f1} = \Delta s + s_{e1} \qquad \theta_{f1} = \theta_{e1} + \Delta\theta_1 .$$

$$s_{f1}^{\ 2} = K1 \cdot s_{f1} \cdot \cos\theta_{f1} + K2 \cdot \sin\theta_{f1} - K3 \qquad (3.2)$$

There are two equations in three unknowns (*K1*, *K2* and *K3*). The free parameter can be used for optimization of the transmission angle.

If deviations of the transmission angles (δ) from 90° at two extreme slider positions are equated, third equation for optimum transmission angle can be obtained.

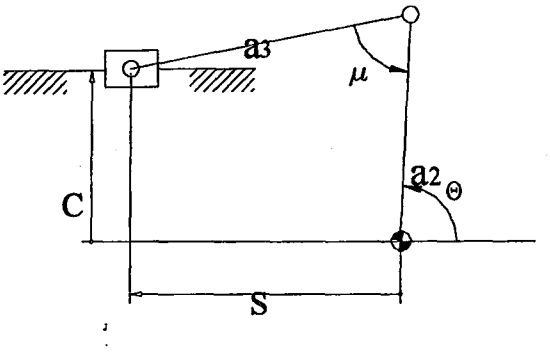

Figure 3.4: Second Slider-Crank

Here, since the input is at the slider, transmission angle is in between the connecting rod and the output-link. The relation between the input displacement s and the transmission angle μ, can be found by cosine law (Figure 3.4):

$$s^2 = -c^2 + a_3^2 + a_2^2 - 2 \cdot a_2 \cdot a_3 \cdot \cos\mu \ .$$

When the first slider-crank is at extended position:

$$s_{e1}{}^2 = -c_1{}^2 + a_3^2 + a_2^2 - 2 \cdot a_2 \cdot a_3 \cdot \cos(\pi/2 - \delta).$$

When the first slider-crank is at folded position:

$$s_{f1}{}^2 = -c_1{}^2 + a_3^2 + a_2^2 - 2 \cdot a_2 \cdot a_3 \cdot \cos(\pi/2 + \delta).$$

Adding the equations above side by side:

$$s_{e1}^2 + s_{f1}^2 = -2 \cdot (c_1^2 - a_3^2 - a_2^2) + 4 \cdot a_2^2 - 4 \cdot a_2^2 \ ,$$

Or,

$$s_{e1}^2 + s_{f1}^2 = K1^2 - 2 \cdot K3. \tag{3.3}$$

Subtracting Equation (3.1) from (3.2), Equation 4 can be obtained:

$$K_2 = \frac{s_{e1}^2 - s_{f1}^2 + K_1 \cdot (s_{f1} \cdot \cos\theta_{f1} - s_{e1} \cdot \sin\theta_{e1})}{\sin\theta_{e1} - \sin\theta_{f1}} \tag{3.4}$$

By substituting *K2* into Equation (3.1), the relation between *K1* and *K3* can be found as:

$$K1 = (K3 + u)/t \tag{3.5}$$

Where:

$$u = s_{e1}^2 + \left(\frac{s_{f1}^2 - s_{e1}^2}{\sin\theta_{e1} - \sin\theta_{f1}} \right) \cdot \sin\theta_{e1},$$

$$t = s_{e1} \cdot \cos\theta_{e1} + \left(\frac{s_{f1} \cdot \cos\theta_{f1} - s_{e1} \cdot \cos\theta_{e1}}{\sin\theta_{e1} - \sin\theta_{f1}} \right) \cdot \sin\theta_{e1}.$$

Substituting *K1* in Eqn. (5) into Eqn. (3), a quadratic equation below can be obtained:

$$K3^2 + K3 \cdot (2 \cdot u - 2 \cdot t^2) + u^2 - t^2 \cdot (s_{e1}^2 + s_{f1}^2) = 0$$

The solution of this quadratic is:

$$K3 = t^2 - u \mp \sqrt{(u - t^2)^2 - u^2 + t^2 \cdot (s_{e1}^2 + s_{f1}^2)} \qquad (3.6)$$

Once *K3* is calculated from Equation (3.6) according to the required swing angle with the initial output-link angle and the initial slider position, then *K1* and *K2* can be easily found from Equations (3.4) and (3.5). According to *K1*, *K2* and *K3* link proportions of the second slider-crank can be easily determined.

3.2.1.2 Determination of the Slider Position for the Second Swing Angle

The second step in the synthesis procedure is to determine slider position for the required second swing angle with the same stroke. At the moment, the link proportions of the second slider is known, the eccentricity and the slider axis of the second slider-crank are the parameters that can only be changed to satisfy the second required swing angle.

Now assume that, when the slider axis is rotated by an angle α, with same stroke, second required swing angle is obtained at the output.

According to the assumption, firstly, Freudenstein's equations must be satisfied for the second required output-link swing angle and the related strokes.

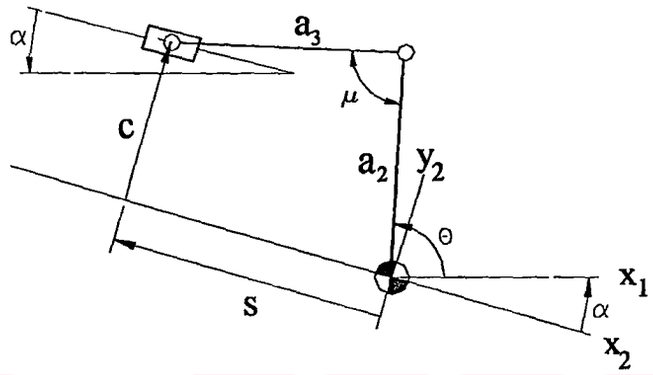

Figure 3.5: Second Slider-Crank at Second Position

According to the new slider axis (parallel to x_2), Freudenstein's equation can be re-written as (Figure 3.5):

$$s^2 + c^2 + 2 \cdot a_2 \cdot (s \cdot \cos(\theta + \alpha) + c \cdot \sin(\theta + \alpha)) = a_3^2 - a_2^2 .$$

Where s and c are defined in the frame 2, and θ is measured w.r.t. x_1.

For the initial output-link angle at the second position:

$$s_{e2}{}^2 + c_2{}^2 + 2 \cdot a_2 \cdot (s_{e2} \cdot \cos(\theta_{e2} + \alpha) + c_2 \cdot \sin(\theta_{e2} + \alpha)) = a_3^2 - a_2^2 \quad (3.7)$$

For the second output-link angle at the second position:

$$(s_{e2} + \Delta s)^2 + c_2{}^2 + 2 \cdot a_2 \cdot ((s_{e2} + \Delta s) \cdot \cos(\theta_{e2} + \Delta\theta_2 + \alpha) +$$
$$c_2 \cdot \sin(\theta_{e2} + \Delta_2 + \alpha) = a_3^2 - a_2^2 \quad (3.8)$$

While switching, since the control-link is rotating around a fixed pivot (Point *A*, in Figure 3.6) the new axis of the slider can't be parallel to its initial axis. After switching, since the first slider-crank proportions don't change, the stroke must be constant for every position of the control link. Therefore, there must be relations between the slider position on the second axis (*AE*) with the switch angle α, the new eccentricity c_2 and the link lengths that synthesized in part 3.2.1.1, for movability of the first slider-crank at the second position. The constraint equations according to these relations must be clearly determined.

The relations between eccentricity, switch angle and initial slider position can be determined from Figure 3.6:

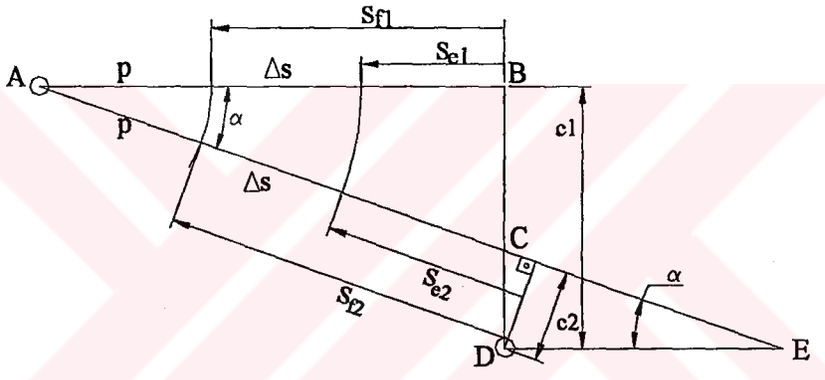

Figure 3.6: Stroke Relations of the Seven-Link Mechanism at two Positions (*A* and *D* are the fixed pivots of the first slider-crank and the second slider-crank respectively)

The relation between second eccentricity c_2 and switching angle α, can be determined as:

$$\frac{|BC|}{|BA|} = \tan\alpha \qquad \left(|BC| = c_1 - \frac{c_2}{\cos\alpha}, |BA| = p + \Delta s + s_{e1}\right)$$

$$c_2 = c_1 \cdot \cos\alpha - (p + \Delta s + s_{e1}) \cdot \sin\alpha, \tag{3.9}$$

The relation between second initial slider position, new eccentricity c_2 and switching angle α, can be determined as:

$$\frac{|AB|}{|AC|} = \cos\alpha \quad |AB| = p + \Delta s + s_{e1},\ |AC| = p + \Delta s + s_{e2} - c_2 \cdot \tan\alpha$$

$$s_{e2} = \frac{(p + \Delta s) \cdot (1 - \cos\alpha) + s_{e1}}{\cos\alpha} + c_2 \cdot \tan\alpha, \tag{3.10}$$

In Equations (3.9) and (3.10) there is a new variable p which is the difference between the connecting rod and the crank of the first slider-crank mechanism. One can eliminate p from Equation (3.10) by using Equation (3.9), to reduce the number of constraint equations by one. However, in this case, p can take many different values, which is not desired. Because the first slider-crank is an in-line type, whose crank length must be half of its stroke. The value of p determines the ratio of the coupler link to the crank, which is the unique parameter that also determines the critical transmission angle. (For in line slider-crank mechanism, the maximum value of the transmission angle is $\mu = \cos^{-1}(b_2/b_3)$). So, in such a case the parameter p must be checked after the synthesis, in order to obtain an appropriate transmission angle for the first slider-crank.

Instead, one can determine the critical transmission angle of the first slider-crank mechanism, which makes the value of p known. Since dimensions of the first slider-crank are functions of stroke Δs and minimum transmission angle μ of the first slider-crank mechanism, the synthesis of the first slider-crank will also be completed. Unless appropriate transmission angles are obtained for the second slider-crank, p can also be used for the optimization of the mechanism with the other free parameters.

For given second output-link swing angle and known first slider-crank dimensions, in Equations (3.7), (3.8), (3.9) and (3.10) there are four unknown parameters; second initial output-link angle θ_{e2}, switching angle α, eccentricity c_2 and second initial slider position s_{e2}. According to unknown parameters, these highly non-linear equations can be solved numerically.

While determining the link proportions according to the first swing angle, initial output-link angle and the initial slider position are arbitrarily selected. In addition, critical transmission angle of the first slider-crank is determined initially. Optimization of the mechanism according to the critical transmission angles can be done by changing these free parameters.

3.2.2 Example 1

Design a seven-link mechanism for 50^0 and 25^0 swing angles.

Let the initial position of the second slider-crank slider be 1.2 times the stroke and let the initial output-link angle be 78°(s_{e1} = 1.2Δs, $\theta_{e1} = 78^0$). Link lengths are found as a_2 =1.1527, a_3 =1.5077 and c_1 = 0.68 from Equations (4), (5) and (6) for 50^0 swing angle. The critical transmission angle deviation for the second slider-crank is 29.3° at first position of the mechanism.

By solving the non-linear Equations (3.7), (3.8), (3.9) and (3.10) numerically for the 25^0 swing angle, the unknown parameters can be found as s_{e2} = 1.19732, α = 24.2°, c_2 = -0.64, θ_{e2} = 113.5°. The critical deviation of the transmission angle from 90° at second position is 29.1°. The value of p is taken as Δs (= 1), that also causes the critical transmission angle deviation of the first slider-crank mechanism to be 19.5°. The ratio of the maximum to minimum link length ratio is 4. The mechanism for two positions is shown in Figure 3.7. The deviations of the critical transmission angles of the second slider-crank are equated to each

other at two positions of the control-link, by simply trying different values of the two free parameters.

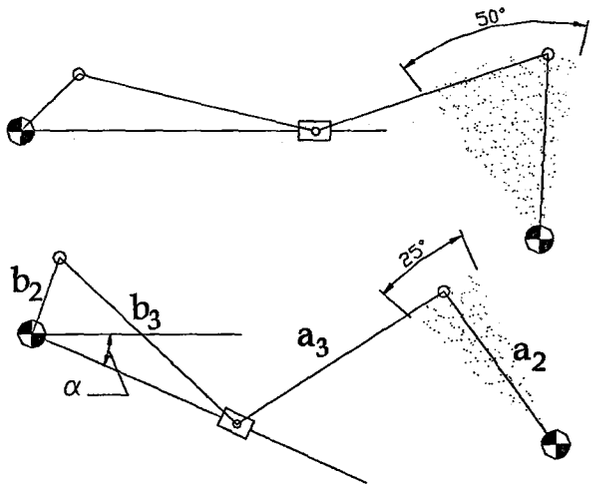

Figure 3.7: A Seven-Link Mechanism for 50^0 and 25^0 Swing Angles

3.2.3 Kinematic Synthesis for three or more Switching Positions

For three or more switching position of the control-link according to the required output-link oscillations, the same synthesis procedure can be used with a simple modification.

Initially, a mechanism can be synthesized according to two extreme output-link oscillations according to the synthesis procedure mentioned in part 3.2.1.1-2. Then by re-solving non-linear equations (3.7), (3.8), (3.9) and (3.10) for the other required output-link oscillations, other switching angles can be determined.

3.2.3.1 Example 2

Design a seven-link mechanism for 50^0, 42^0, 33^0 and 25^0 swing angles.

The mechanism synthesized for 50^0 and 25^0 Example 1 can also be used in this example since the extreme oscillations are the same. By re-solving Equations (3.7), (3.8), (3.9) and (3.10) for the angles 42^0, 33^0 corresponding switching angle and eccentricity can be determined as, $\alpha = 10.5°$, c = 0.4306 and $\alpha = 17.98°$, c = -1.7056 respectively. The critical transmission angle deviations at these positions are 34.7° and 33.4°.

According to the same kinematic synthesis technique, by increasing the swing angle and the difference between first and second swing angles, the limit of this type of variable structure can be determined.

Some of the mechanisms are shown in Table 1.

Table 1: Link Proportion of Variable Structure Mechanisms (ctad stands for critical transmission angle deviation)

	1	2	3	4	5
$\Delta\theta_1/\Delta\theta_2$	50°/25°	70°/30°	90°/65°	110°/85°	120°/90°
a_2	1.1527	0.864	0.707	0.566	0.56
a_3	1.5077	1.203	1.5	2.3174	1.6203
c_1	0.68	0.6038	0.5	1.166	0.6627
c_2	-0.64	-0.292	-0.4986	-1.16	-0.6564
α	24.2°	19.9°	18.6°	32.2°	24.8°
ctad #1	29.3°	37.1°	45°	50.4°	55.7°
ctad #2	29.3°	37.6°	45°	50.7°	56°

During the synthesis of these mechanisms, the stroke is taken unity. First slider crank proportions are $b_2 = 0.5$ and $b_3 = 1.5$ unit for all mechanisms. The coupler-link dimension of the first slider-crank (or the parameter *p)* has a very slight effect on transmission angle of the second slider-crank. Therefore, initially the coupler-link is taken as three times of the crank, which makes the maximum

deviation of the transmission angle of the first slider-crank mechanism 19.5°. The control-link length is taken as $b_2+b_3=2$ unit for all mechanisms.

Fifth mechanism is an example of limit of this type of variable structure mechanisms. The critical transmission angle deviation at the second position is 56°.

Among all of the mechanisms in the table, the worst of the maximum to minimum link length ratio is four, which is a good result.

3.3 Synthesis Procedure for the Second Type of Seven-Link Mechanism

In this part, a synthesis procedure for the second type of variable structure mechanism will be developed (Figure 3.8). The approach is similar to the one, which was developed for the first type of variable structure mechanism. The general properties of this variable stroke mechanism are mentioned in part 3.1.

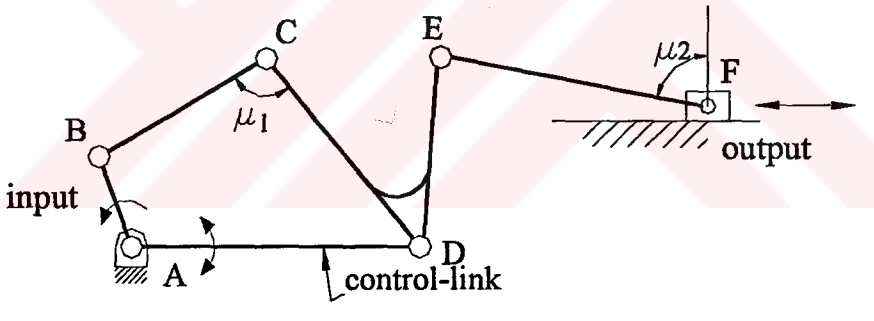

Figure 3.8: Variable Stroke Mechanism

The synthesis of the seven-link mechanism (Figure 3.8) will be performed in two steps according to the required two different output strokes. Initially, a slider-crank will be designed for the larger stroke. Then, considering the constraints, second position of joint *D* will be determined to obtain the smaller required stroke with the same input swing angle for link *ED*. At the last step the four-bar mechanism, which is a crank-rocker type will be easily synthesized according to known parameters.

During synthesis, the two transmission angles must be considered, are shown in Figure 3.8 as, μ_1 and μ_2

3.3.1 Formulation of the Second Type of Seven-Link Mechanism

3.3.1.1 Determination of the Link Proportions According to the First Swing Angle

Initially, the slider-crank will be designed for arbitrarily selected initial crank angle, initial slider position and crank oscillation for unit stroke, when the four-bar is at folded position.

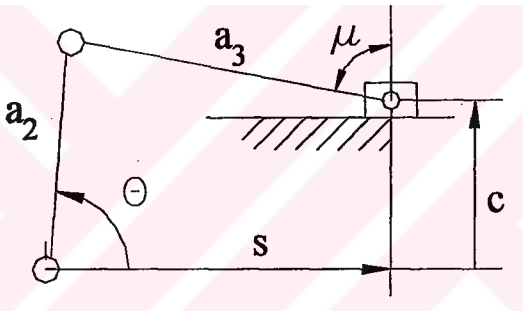

Figure 3.9: Slider-Crank at the First Position

Freudenstein's equation for the slider-crank mechanism is:

$$s^2 = K1 \cdot s \cdot \cos\theta + K2 \cdot \sin\theta - K3$$

Where:

$$K1 = 2 \cdot a_2, \quad K2 = 2 \cdot a_2 \cdot c, \quad K3 = a_2^{\,2} - a_3^{\,2} + c^2$$

When the four-bar is at folded position:

$$s_{f1}{}^2 = K1 \cdot s_{f1} \cdot \cos\theta_{f1} + K2 \cdot \sin\theta_{f1} - K3 \qquad (3.11)$$

When the four-bar is at extended position:

$$s_{e1}{}^2 = K1 \cdot s_{e1} \cdot \cos\theta_{e1} + K2 \cdot \sin\theta_{e1} - K3 \,. \qquad (3.12)$$

Where:

$$s_{e1} = s_{f1} + 1 \quad \text{and} \quad \theta_{e1} = \theta_{f1} - \Delta\theta \,.$$

In Equations (3.11) and (3.12), there are three unknowns (*K1*, *K2* and *K3*). Then the free parameter can be used for the optimization of the transmission angle. According to the Figure 3.9 the relation between crank angle and transmission angle can be determined as:

$$a_2 \sin(\theta) - a_3 \cos(\mu) = c_1 \qquad (3.13)$$

If the deviations of the transmission angles from 90° at two extreme slider positions are equated, the third equation for the optimum transmission angle can be obtained. When the four-bar is at extended position the transmission angle is $\mu_{e1} = \pi/2 + \delta$ and when the four-bar mechanism is at folded position the transmission angle is $\mu_{f1} = \pi/2 - \delta$. From Equation (3.13), by eliminating δ, Equation (3.14) can be obtained.

$$a_2(\sin\theta_{e1} + \sin\theta_{f1}) = 2c_1 \,,$$

Or,

$$\sin\theta_{e1} + \sin\theta_{f1} = 4K_2/K_1^2 \,. \tag{3.14}$$

From Equations (3-11,12 and14), Eqn. (3-15) can be obtained:

$$\begin{aligned} K1 &= \frac{-v \pm \sqrt{v^2 + 4uyz}}{2yz}, \\ K2 &= zK_1^2, \\ \mathrm{K3} &= -s_{f1}^2 + K_1 s_{f1}\cos(\theta_{f1}) + K_2\sin(\theta_{f1}) \end{aligned} \tag{3.15}$$

Where:

$$\begin{aligned} u &= s_{f1}^2 - s_{e1}^2, \\ \mathrm{v} &= \mathrm{s_{f1}}\cos(\theta_{f1}) - s_{e1}\sin(\theta_{e1}), \\ \mathrm{y} &= \sin(\theta_{f1}) - \sin(\theta_{e1}), \\ \mathrm{z} &= (\sin(\theta_{e1}) + \sin(\theta_{f1})/4 \,. \end{aligned}$$

According to *K1*, *K2* and *K3* link proportions of the slider-crank mechanism can be determined for unit stroke.

3.3.1.2 Determination of the Crank's Floating Pivot Position of the Slider-Crank for the required Second Stroke:

At the second position of the control-link, the eccentricity of the slider-crank mechanism changes therefore the output stroke changes.

Assume that if link b_1, the fixed link of the four-bar, is rotated by an angle α, second required stroke is obtained.

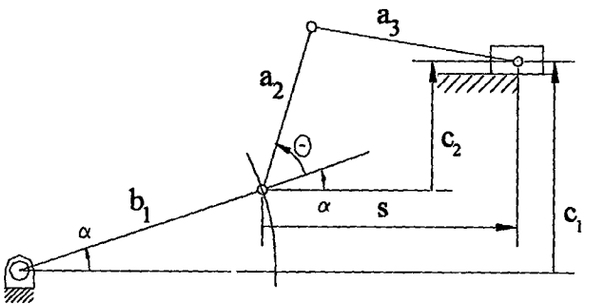

Figure 3.10: Mechanism at the Second Position

According to assumption above, Freudenstein's equations must be satisfied for the required second stroke. For the second position of the control link Freudenstein's equation can be re-written as:

$$s^2 + c^2 + 2 \cdot a_2 \cdot (s \cdot \cos(\theta + \alpha) + c \cdot \sin(\theta + \alpha)) = a_3^2 - a_2^2 .$$

Link proportions of the four-bar mechanism remains the same for all positions of the control-link. The output-link angle of the four-bar mechanism at extended and folded positions also remains the same with respect to the axis, which is collinear with link b_1. Therefore, for the second position of the control-link, corresponding crank angles for extreme slider positions are:

$$\theta_{e2} = \theta_{e1} + \alpha \quad \text{and} \quad \theta_{f2} = \theta_{e2} + \Delta\theta. \tag{3.16}$$

In addition, constraint equations must be clearly stated. According to Figure 3.10 the relation between eccentricity at second position with the switching angle and the fixed of the four bar mechanism is:

$$c_2 = c_1 - b_1 \cdot \sin\alpha \tag{3.17}$$

Substituting Equations (3.16) and (3.17) into Freudenstein's equations for the two extreme slider and corresponding crank angle positions, equations that satisfies the required stroke are obtained as:

$$s_{e2}^2 + (c_1 - b_1 \sin\alpha)^2 - 2a_2 (s_{e2} \cos(\theta_{e1} + \alpha) + (c_1 - b_1 \sin\alpha) \sin(\theta_{e1} + \alpha) = a_3^2 - a_2^2 \tag{3.18}$$

$$(s_{e2} - \Delta s_2)^2 + (c_1 - b_1 \sin\alpha)^2 - 2a_2 ((s_{e2} - \Delta s_2) \cos(\theta_{e1} + \Delta\theta + \alpha) + (c_1 - b_1 \sin\alpha) \sin(\theta_{e1} + \Delta\theta + \alpha) = a_3^2 - a_2^2 \tag{3.19}$$

Analytical solution of highly non-linear Equations (3-18, 19) for the unknown parameters isn't possible. Therefore, these equations will be solved numerically to determine the fixed link of the four bar b_1 and the switching angle α. Here, the slider position at the extended position s_{e2} is a free parameter. Therefore, the number of free parameters increases to four.

If the slider positions at extended positions are required to be the same at two positions of the control-link, according to Figure 3.10, Equation (3.20) must also be satisfied:

$$s_{e2} = b_1(1 - \cos\alpha) + s_{e1} \tag{3.20}$$

When Equation (3.20) is substituted into Eqns. (3.18) and (3.19), the number of unknowns and equations will be equal.

3.3.1.3 Synthesis of the Four-Bar

The last step in synthesis procedure is to design the four-bar mechanism. Centric crank-rocker type four-bar can be used to obtain optimum transmission angle. Note that, fixed-link b_1 and output-link swing angle $\Delta\theta$, of the four-bar are determined in part 3.3.1.1-2.

According to Brodell and Soni's analytical method for the centric crank-rocker mechanism, the link lengths can be determined as:

$$
\begin{aligned}
b_3 &= b_1\sqrt{\frac{1-\cos\Delta\theta}{2\cos^2\mu_{\min}}} \\
b_4 &= b_1\sqrt{\frac{1-(b_3/b_1)^2}{1-(b_3/b_1)^2\cos^2\mu_{\min}}} \\
b_2 &= b_1\sqrt{(b_3/b_1)^2+(b_4/b_1)^2-1}
\end{aligned}
\tag{3.21}
$$

In Equations (3.21), there is a new free parameter μ_{min}, which is the minimum value of the transmission angle of the four-bar. With this parameter, the number of free parameter increases to five at the end of synthesis procedure.

The mechanism can be optimized by trial and error to obtain appropriate transmission angles and link proportions.

3.3.2 Example 3:

Design a variable-stroke mechanism for sixty-percent stroke at second position.

Let the initial free parameters, crank oscillation is $\Delta\theta = 50^0$, slider-position at extended position is $s_{e1} = 2.7$ and corresponding crank angle is $\theta_{e1} = 52^0$. According to Equations (3-15), link proportions of the slider-crank mechanism is a_2

=1.214, a_3 =1.956 and c_1 = 1.072. (The stroke of the slider-crank is taken as unity). The maximum deviation of the transmission angle from 90^0 for the slider-crank is 4,2° at first position of the mechanism.

By solving non-linear Equations (3.18,19) numerically (the free parameter, slider position at extended position s_{e2}, is taken 2.7 unit), the unknown parameters, switching angle and control-link length at the second position are determined as, α = -21.5°, b_1 = 1.607 respectively. Also according the Equation (3-16), eccentricity at second position c_2 is 1,661. In the second position, the maximum deviation of the transmission angle from 90° is 32.2°.

In the last step, link proportions of the four-bar mechanism for the known swing angle and the fixed link length can be synthesized according to Equations (3.29). Where b_2 = 0.565, b_3 = 1.057, b_4 = 1.336 (The last free parameter, minimum transmission angle of the four bar mechanism is taken 50^0).

Maximum to minimum link ratio is 3.47.

The mechanism for two position of the control-link is shown in Figure 3.11.

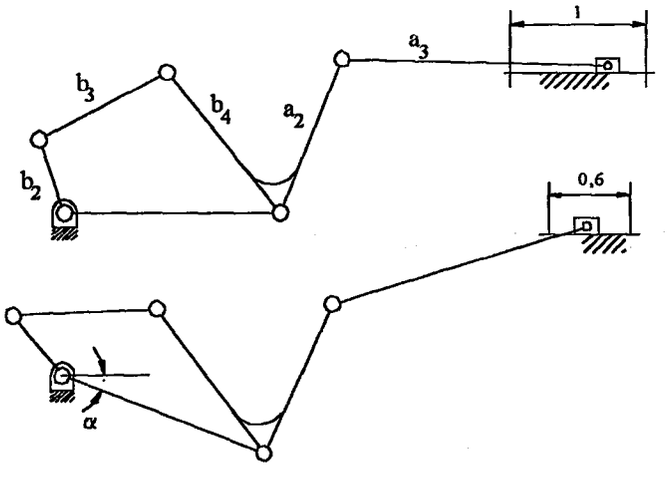

Figure 3.11: Variable Stroke Mechanism for 60 % Stroke at the Second Position.

Position of the slider vs. crank angle is shown in Figure 3.12. (Kinematic analysis of this type of variable structure mechanism is not mentioned in this study). The dashed line curve represents second position of the mechanism.

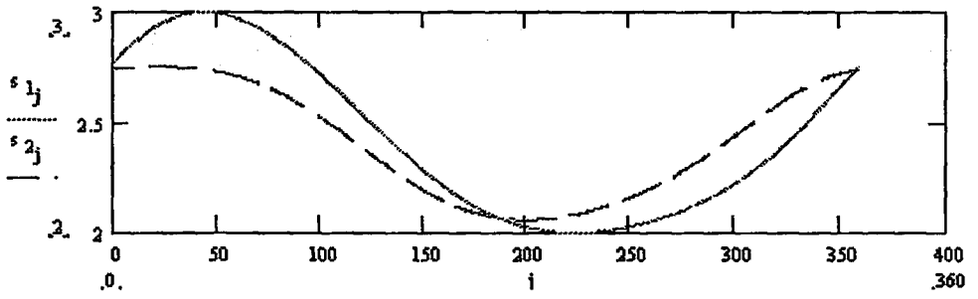

Figure 3.12: Slider position vs. Crank Angle for two positions

CHAPTER 4

SWITCHING ANALYSIS OF VARIABLE STRUCTURE MECHANISMS

4.1 Introduction

The motion of the control-link of the variable structure mechanism to another pre-determined position to satisfy the required second oscillation is named as "Switching". The first type of variable structure mechanism is taken into consideration, to explain a procedure for this phenomenon.

Switching can be performed in several ways, in this study, in order to obtain a low-cost mechanism, the advance of the control-link from one position to another without using an external control will be investigated. For example, when the mechanism is working at its first position, if there is a sudden increase in the output-link torque during forward stroke the mechanism will switch to other position (smaller output-link oscillation position). Moreover, when the output-link torque decreases to a specific value the mechanism will switch back to its first position. This type of switching can be called as "Automatic Switching". A mechanical logic element will be integrated to the control-link of the variable structure mechanism to perform automatic switching.

For low-speed operations, static force analysis and for high-speed operations dynamic force analysis will be done to investigate appropriate switching conditions.

4.2 Switching Analysis for Low-Speed Operations

For low-speed operations since the inertia forces due to link masses are so small, static force analysis is enough to determine the torque applied to the control-link.

Before the static force analysis, position analysis of the seven-link mechanism must be done. In addition, movability of the mechanism can be checked for all input crank angles.

Position analysis of the mechanism is shown in Appendix-A.

According to the force analysis procedure given in Appendix-B, the torque applied to the control-link can be determined.

Since both values of the input and the output-link torque are unknown, some assumptions must be done.

The input motor torque from crank a_2 and the output-link torque due to work done are the forces that are applied to the mechanism externally. In the forward stroke (clockwise), a constant and unit resistive torque opposite to angular velocity of the output-link is assumed. In the reverse stroke (counter clockwise), the resistive torque is assumed to be one fifth of the unit torque, again, opposite to the angular velocity of the

output-link. The torque from the input motor is such that the mechanism is at static equilibrium at all positions. During switching the output-link remains stationary, while the crank is rotating.

If the threshold torque of the switch key on the control-link is set to a suitable value, switching may occur.

The conditions that must be satisfied for switching are:

1- Resultant torque that applied to the control-link must be along to the required direction of rotation, both at the instant of the start of the switching and during switching.

2- Same output-link angle must exist for both position of the control link at the switching position. Because, during switching the output-link remains stationary while crank is rotating.

4.2.1 Example 4

Determine the threshold torque values of the switch key and the corresponding crank angles of the mechanism that synthesized in Example 1, for switching at two positions.

Kinematic analysis of this mechanism is performed according to the position analysis procedure given in Appendix-A. Oscillation of the output-link vs. input crank angle of the mechanism is shown in Figure 4.1:

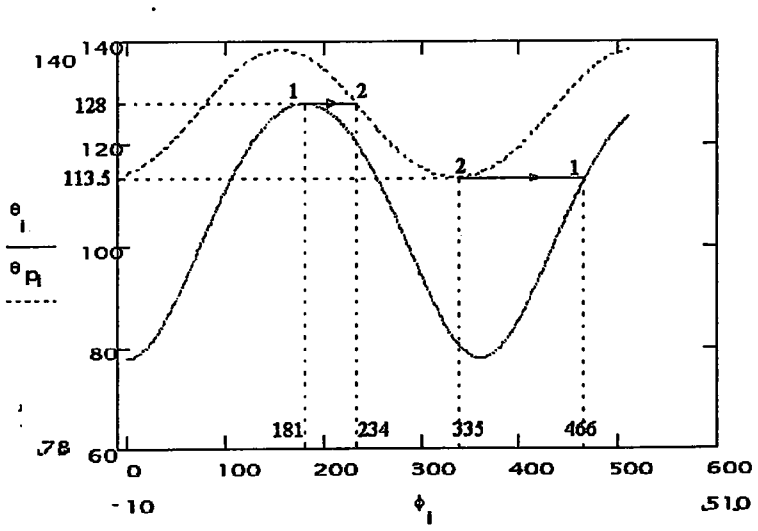

Figure 4.1: Output-Link Angle vs. Crank Angle

As it is seen from Figure 4.1, switching may occur when the output-link angle is in between 113.5° and 128°. Because except this interval the same output-link angle doesn't exist for two positions of the mechanism. (The output-link position doesn't change during switching). Corresponding crank angles for this interval are; 106.5°<ϕ< 253.5° at the first position, 0°<ϕ<78° and 232°<ϕ<360° at the second position of the mechanism. (The dashed line curve is obtained at second position)

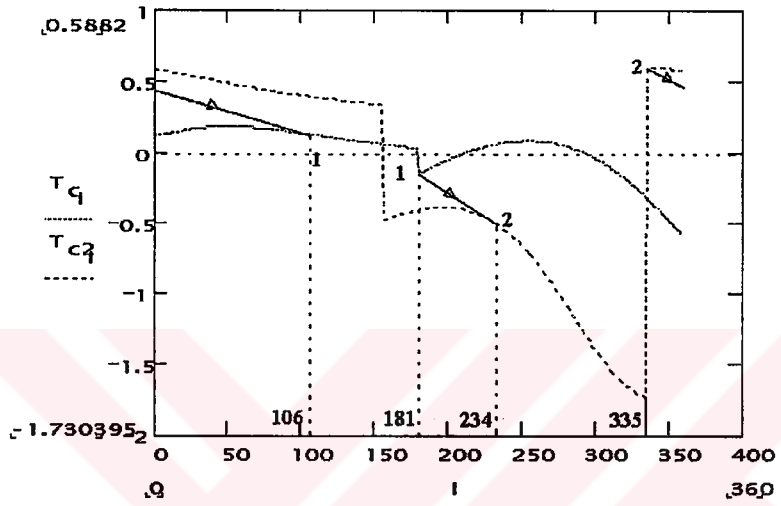

Figure 4.2: Torque Applied to the Control-Link from the Slider

The torque applied to the control-link at two positions is obtained from Equation (B.9) as a function of the crank angle and it is shown in Figure 4.2. (The dashed line curve is obtained at the second position of the mechanism)

While switching from first to second position, the control-link must rotate in clockwise direction. The requirements for switching to the second position are; the torque must be negative (CW) at start of the switching and during switching, the crank angle must be in between 106.5°<ϕ <253.5°. These requirements are simultaneously satisfied in the region 181°<ϕ < 211°. However, in this interval the torque curve starts from –0.15 unit (When ϕ = 181°) and its absolute value always decreases. Therefore, switching must start at crank angle ϕ = 181°.

If another crank angle were selected for the start of switching, for example 189°, the threshold value of switch key would be set to 0.1 unit. Since the torque applied on the control-link exceeds 0.1 unit at 181° crank angle (0.15 unit), switching again would start when the crank reaches to 181°

Similarly, requirements for switching from the second to the first position are; the torque must be positive (CCW) at start of the switching and during switching, the crank must be at $0°<\phi<78°$ and $232°<\phi<360°$. These requirements are satisfied in $-24°<\phi<78°$ crank angles simultaneously. Again, in this interval the torque curve starts from 0.38 unit ($\phi = 337°$) and its value always decreases. Therefore, switching must start at crank angle $\phi = 337°$. After the crank reaches to 106.5°, switching will end. At this crank position, the torque applied on the control-link is +0.18 unit.

According to switching analysis of the seven-link mechanism that synthesized in Example (1), the starting positions of switching crank angles are unique.

Note that, when $316°<\phi<360°$, the control-link torque at the first position is greater than the threshold value ($T > 0.15$) defined for switching to second position. Under this condition, the control-link torque exceeds the threshold value when $316°<\phi<360°$ and where the corresponding output-link doesn't exist for the second position. Normally, undesired switch motion starts and the mechanism locks in this interval. To overcome this problem, the torque applied to control-link in the region where switching isn't required may be decreased under the threshold value by changing the free parameters in the synthesis. Briefly, obtaining an appropriate torque curve can also be an optimization objective. However, many trials showed that it is not always possible to obtain a torque curve as required with appropriate transmission angles and reasonable link ratios.

As another alternative, a simple modification to mechanism can be done whenever such a problem exists. The friction force between the control-link and the fixed-link can be increased only in the interval required by a mechanical element. This modification is mentioned in part 4.2.2

4.2.2 Modification of the Mechanism

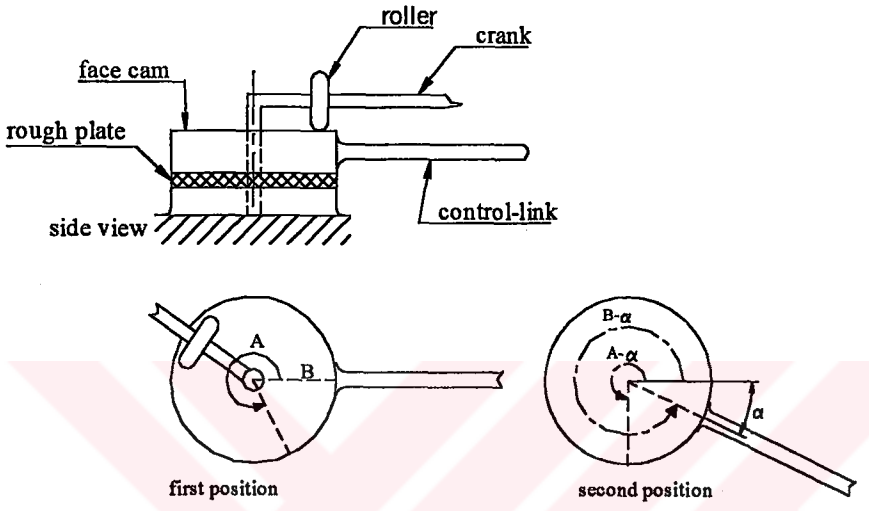

Figure 4.3: Modification

Increase in the friction force of the control-link, where needed, can be done by means of a face cam attached to control-link and a roller follower mounted on the crank as shown in Figure 4.3.

The profile of the face cam has a rise at angle A and where return is ended at angle B (dashed line portion) as shown in Figure 4.3 (top view). When the crank reaches to the start of region where friction force is required (*A*), since the profile starts a rise, the pressure between elastic rough plate and the control-link and the friction force increases. This pressure increase continues up to angle *B*. If the lift of the profile is set to an appropriate value, unwanted movement of the control-link will be prevented. Outside the dashed line portion, there is no rise in the profile; in other words, the dwell region is present. In this portion, the normal force between control-link and the rough plate is zero hence switching is possible.

When the control-link torque curve obtained for the mechanism that synthesized in Example 1 is considered, in the first position, the threshold is set to a specific value in *X* (Figure 4.4). Since in between *A* and *B*, the control-link torque is greater than the threshold value at *X* the friction force must be increased to prevent switching in this interval. When crank is on *A*, the rise of the cam can start and the return should be ended at *B* (Figure 4.4). So the control-link will always remain stationary in between *A* and *B*.

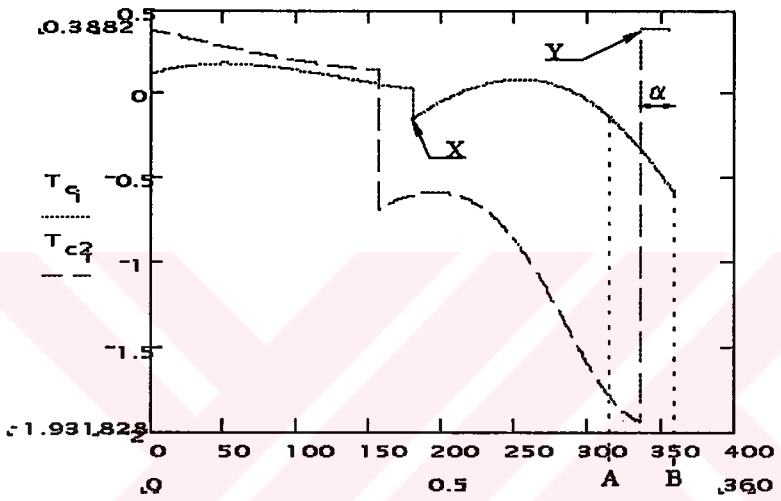

Figure 4.4: A Typical Control-Link Torque Diagram

In the second position, switching back to first position occurs at *Y* (Figure 4.4). It looks like point *Y* is in between *A* and *B* where the friction force is increased, but since the control-link (also the face-cam) rotates in clockwise direction by angle α after switching, this is not true. Because in the second position as shown in Figure 4.4 the dashed line portion is in between A-α and B-α with respect to crank angle position. Therefore, at the second position, *Y* is out of the dashed line portion and this is required for switching back to first position.

Note that, since there is a resistive torque at the output-link for forward and reverse strokes (causes a direction change in output-link torque), there must be a jump in torque curves at the end of both strokes. In addition, many trials showed that switching from one position to another starts at the beginning of a stroke. (*X*

and Y in Figure 4.4) Also, the control-link rotates by an angle α, the extreme slider positions that specify stroke limits with respect to crank angle will be shifted by angle α (shown in Figure 4.4). So inherently, at the second position switching is not prevented by the brake system, which is required for the first position.

Consequently, with the brake system integrated to control-link when the external torque applied to output-link exceeds a certain value the mechanism can switch automatically to low oscillation (second) position at only specified position conveniently.

Generally, for variable structure mechanisms, if switching first to second position occurs during the forward stroke of the output-link, switching back to first position occurs during the reverse stroke or vice versa. As in Example 4, switching second to first positions may occur during the reverse stroke ($180-\alpha < \phi < 360-\alpha$), where switching is not as simple as in the forward stroke. Because, in this example during the reverse stroke the work done is against the friction force and in a normal application, friction force does not change. Therefore, the control-link torque curve during the reverse stroke won't be effected when the output-link load decreases or increases. Under this condition, switching back to first position is not possible.

In addition, there is one more problem with automatic switching; at second position where the output-link oscillation is smaller, switching is required when the external torque at the output-link decreases under to a specific value. According to Equation (B.9), magnitude of the control-link torque is linearly proportional to the output-link torque. Therefore, if the torque at the output decreases, the control-link torque will also decrease. However, switching can start only if, when the torque applied to control-link increases over threshold value of the switch key. Consequently, when the external output torque decreases, again switching is not possible.

To overcome these problems the two possible ways are:

1- The mechanism can be modified (Mentioned in part 4.2.3)

2- Mechanism can always switch back to first position after forward stroke at the second position regardless of the output-link torque value. Nevertheless, in such a case there will be considerable amount of work loss during forward stroke at second position. According to Figure 4.2, if the mechanism always starts to perform work at point 2 (after switching, the mechanism can start to do work at this point), there will be a considerable amount of work loss. In this example, forty percent of the forward stroke can't be used.

4.2.3 Second Modification of the Mechanism

Firstly, since the output-link torque varies only in the forward stroke where the work is done, switching back to first position must be investigated in the forward stroke. However, according to the control-link torque curve of the mechanism synthesized in Example 4, during the forward stroke at the second position the direction of the torque applied to control-link is always in clockwise (negative) direction (Figure 4.2). At the second position the control-link must rotate in counter clockwise (positive) direction to switch to first position therefore, the torque applied to control-link must be in this direction.

Now, if a spring (torsional or bending type) is attached between the control-link and the fixed-link, which applies counter clockwise torque to the control-link at second position, the torque characteristics of the control link can be changed. The spring will be mounted on this link so that spring force at the first position will be zero in order not to disturb switching at first position. In order to obtain an increase at the control-link torque, when there is a decrease at the output torque, the following procedure can be used:

The torque applied to control-link from slider will be opposite to the desired direction for switching. The spring exerts a force to the control-link in desired switching direction. Consequently, the total of spring force and torque from the slider will increase in desired direction of rotation when there is a decrease in the output torque.

4.2.4 Example 5

According to Figure 4.4, at second position when crank angle is 245^0, the torque applied to control link is -0.6 unit for one unit external torque at the output-link. Assume that, a spring attached to control-link exerts +0.8 unit torque to the control-link. The total torque applied to control-link will be +0.8+(-0.6) = +0.2 unit. So, totally a positive control-link torque is obtained. Then, let the threshold value of the switch key is 0.3 unit. Now, if the external output-link torque decreases below one unit, for example 0.7, according to Equation (B.9) at this crank angle (245^0) the torque applied to control-link from slider will be –0.42 unit. So, with the spring force, the total torque will increase to +0.38 unit (+0.8+(-0.42)) which is larger than the threshold of the switch key (0.3 unit) and switching will start. (Switching second to first position can't be realized in between 180-α and 360-α. Because, the control-link starts to rotate first in clockwise direction for while during switching then the mechanical stoppers obstructs this movement and the mechanism may lock. However, the procedure of switching when there is a decrease at the external torque can only be applied in this region for the mechanism taken into consideration)

Consequently, with a simple spring attached to the control-link, the direction of the control-link torque can be changed and when there is a decrease in the output-link torque, an increase at the control-link torque can be obtained simultaneously.

Note that, according to the torque curve at the second position in Figure 4.4, at the region where positive torque is larger than the switch-key threshold (+0.3), friction force must be increased according to the method mentioned in part 4.2.2.

If the modifications mentioned in parts 4.2.2 and 4.2.3 are done to the mechanism appropriately, automatic switching to both positions under varying load conditions at the output-link may be possible. However, another alternative for switching, using an electrical switch at the control-link, which is controlled externally, comes into consideration, as the modification procedure becomes complicated. Because at the beginning of the study, the objective is to obtain a low cost and simple mechanism that can switch automatically. Nevertheless, without any modification, it seems to be impossible to obtain such a mechanism.

4.3 Switching Analysis for High-Speed Operations

Static analysis of the seven-link mechanism is valid only at low-speed operations. At high-speed applications since the effect of inertia forces increase, dynamic analysis of the mechanism must be done.

Switching one position to another will be investigated in two parts. Initially, appropriate crank position will be determined for start of switching, then after the control-link releases from switch-key dynamic characteristics of the mechanism must also be investigated in order not to lock the mechanism. Because unlike low-speed operations, at high-speed operations inertia forces may cause an undesired motion of the output-link and the same output-link position isn't present for all crank angles at two positions.

During the dynamic analysis, for reducing the complexity of algebraic solution of the mechanism, concentrated mass approach will be used. In addition, angular velocity of the input crank is assumed constant during switching.

Firstly, velocity and acceleration analysis of the mechanism must be done for the force analysis. This analysis is given in Appendix-C.

After acceleration analysis, by dynamic force analysis the control-link torque for two positions can be determined as given in Appendix-D.

Similar to low-speed switching analysis, in the forward stroke (clockwise), a constant, resistive torque opposite to angular velocity of the output-link is assumed. In the reverse stroke (counter clockwise), the resistive torque is assumed to be one fifth of the unit torque again opposite to the angular velocity of the output-link.

During the low-speed switching analysis, due to the problems for automatic switching, some modifications are taken into consideration. However, in high-speed analysis since inertia forces are also effective, especially during switching, controlling the motion of the mechanism isn't as simple as in the low-speed operations. Therefore, for a convenience in switching, in the dynamic analysis it is assumed to have an electrical switch, which is externally controlled. This switch will release the key with an external signal when desired.

4.3.1 Example 6

Determine the position of the start of switching to both positions for the mechanism that have link lengths as $a_2 = 145.4$, $a_3 = 211.3$, $c_1 = -10.71$, $b_2 = 75$, $b_3 = 188$, $\Delta s = 150$ and the switching angle $\alpha = 18.4^0$. ($s_{e1} = 170$ where $\theta_{e1} = 100^0$). At the output-link two different swing angles, 50^0 and 25^0, are obtained. The critical transmission angle deviations at the first and second position of this mechanism are 36.7^0 and 43.7^0. (For high-speed switching, for convenience, when control-link releases from its switch key, some conditions must be satisfied. These conditions will be mentioned in part 4.3.2 and this mechanism is optimized due to the requirements related to this part)

The input crank speed is 200 rpm. Mass per unit length of the links is ½ kg/m. The centers of gravity of the coupler links of the first and second slider-crank are close to their crankpin as an amount of L/3. The slider mass is assumed 0.1 kg.

The external torque applied to output-link during the forward stroke (clockwise) is 10 N.m. During the reverse stroke one fifth of this value, 2 N.m. resistive torque, applied to the control-link is assumed.

Position analysis of this mechanism is performed according to the procedure mentioned in Appendix-A. Oscillation of the output-link vs. input crank angle of the mechanism for two positions is shown in Figure 4.5:

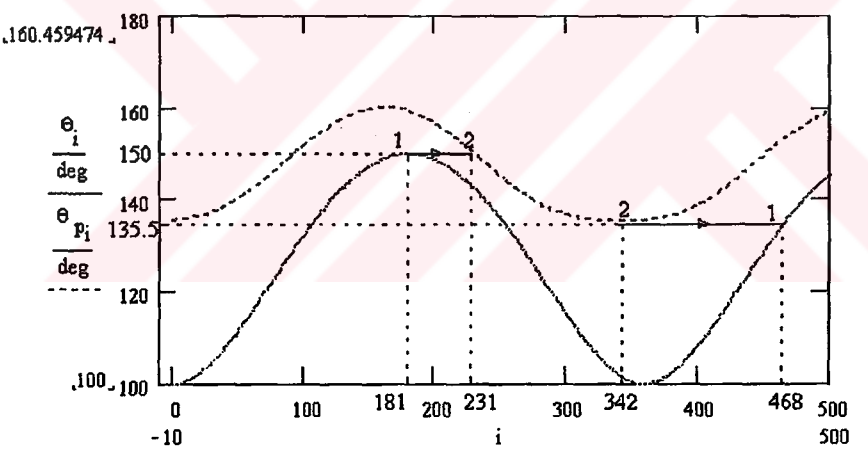

Figure 4.5: Output-Link Angle vs. Crank Angle

According to the analysis procedure given in Appendix-C, velocity and acceleration of the output-link vs. crank angle at two different positions are determined for 200 rpm crank speed and shown in Figure 4.6.

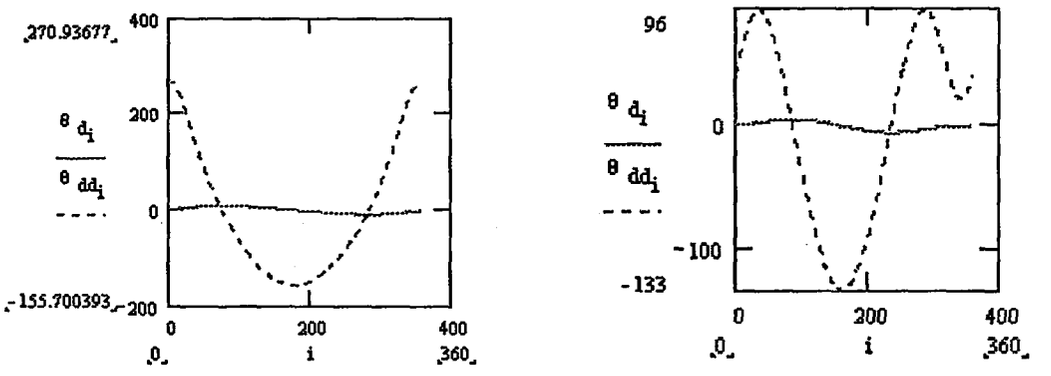

Figure 4.6: Output-link Velocity and Acceleration for two Positions

In Figure 4.6, the figure in left refers to first, the right one refers to second position of the mechanism. In these figures, the dashed line curve represents acceleration and the continuos line represents the velocity of the output-link.

By using Equations (D.4) and (D.5) the concentrated mass portions can be determined as (Figure D.1); m_C = 0.166 kg and m_D = 0.1 kg and the moment of inertia of the output-link w.r.t E is 2×10^{-3} kg.m^2.

From Equation (D.10), the torque applied to the control-link at two positions can be determined. These torque curves is shown in Figure 4.6. The continuos line refers to the first, dashed line refers to the second position.

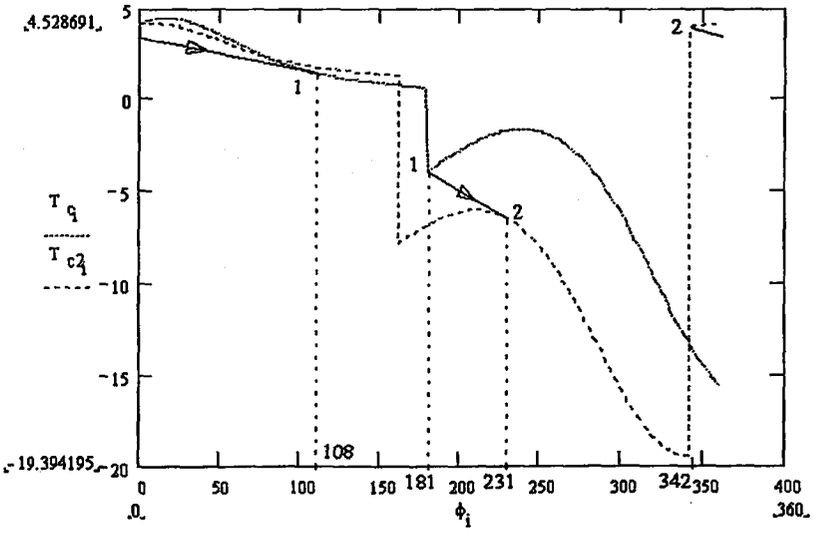

Figure 4.7: Torque Applied to the Control-Link from the Slider

If a comparison is done between the control-link torque curve obtained in Figure 4.2 (for low-speed oper.) and the one in Figure 4.7, the similarity is clearly seen. Then for start of switching, the similar crank positions can be used. These positions are

shown in Figure 4.5 and 4.7. At the first position, when desired, the switch can take a signal when the crank angle is 181^0 and the control-link will start to move in clockwise direction. Because, according to the curve in Figure 4.6, the torque applied to control-link is in clockwise direction (-3.9 N.m.). Similarly, at the second position, the switch will take a signal when the crank angle is 342^0 and the control-link will start to move in counter clockwise direction. The corresponding value of the torque applied to control-link is +4 N.m.

Up to now, the dynamic switching is similar with the low speed-switching analysis. However, at this point, the motion of the mechanism must be investigated so that the mechanism does not lock during switching since unlike the static case, the output-link may not remain stationary.

4.3.2 Analysis of the Mechanism during Switching

In Example 6, for the start of switching, at first position 181^0 crank angle is specified and at the second position 342^0 is specified despite there are other crank positions present that satisfies the direction requirement for the control-link torque. Because at these crank angles the first slider-crank mechanism is in folded and extended positions where the slider velocity therefore the output-link's angular velocity is zero.

Since there is a resistive external torque for both positions of the mechanism, there is a possibility to keep the output-link motionless during switching. If this requirement is satisfied, the mechanism can switch in a convenient way. If another position is specified rather than the dead positions of the crank, the

output-link's angular momentum will not be zero. Under this condition, a detailed analysis of the two degree-of-freedom dynamic system must be performed in the switching region. There may be a possibility to obtain such a switch motion in theory, but since this is a very fine operation, due to the manufacturing and operation condition imperfections, real model may not work as desired. Therefore, switching will be investigated while the output-link is stationary for both at the instant of switching and during switching.

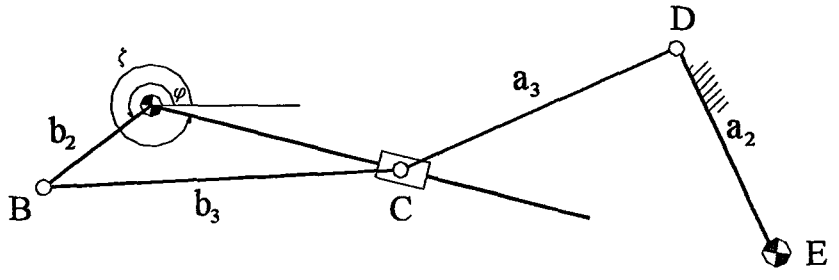

Figure 4.8: Mechanism during switching

During switching, if the output-link is required to be stationary while the control-link is moving to its other position, the six-link mechanism shown in Figure 4.8 must be investigated. Point *D* can be assumed as the fixed pivot of the mechanism.

During switching, in order to determine whether the output-link will remain steady or not, force analysis of the mechanism must be performed. (If the torque applied to the output-link from link a_3 is smaller than the resistive external torque, output-link also remains stationary during switching) Before the force analysis, kinematic analysis of the six-link mechanism (Figure 4.8) during switching must be performed. The movability of the mechanism can be checked after the position analysis. Position, velocity and acceleration analysis of the mechanism obtained during switching is given in Appendix-E.

4.3.3 Example 7

Analyze the mechanism in Example 6 for both positions whether its control-link remains steady or not during switching.

Initially switching first to second position will be investigated. According to Figure 4.5, crank rotates from 181^0 to 231^0 when output-link is assumed to be steady, for switching first to second position.

Position, velocity and acceleration analysis of the mechanism is done according to Appendix-E and the control-link's analysis is shown in Figure 4.9.

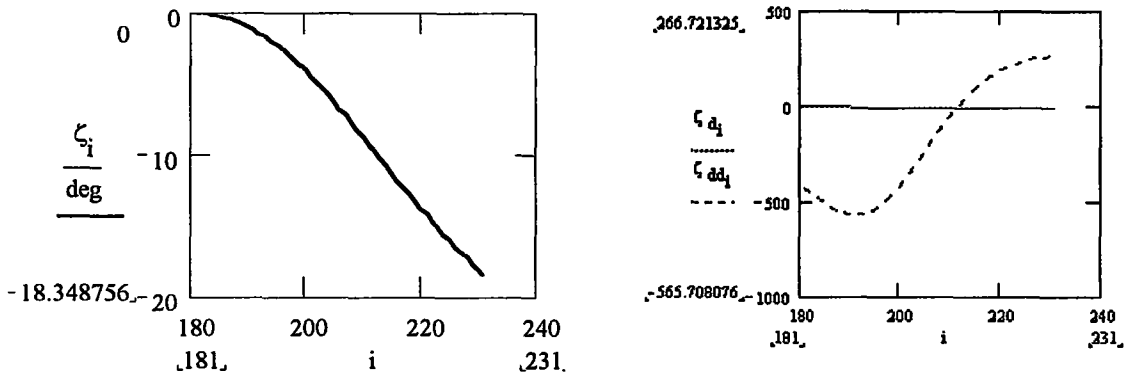

Figure 4.9: Position, Velocity and Acceleration of the Control-link

After the kinematic analysis, the force analysis is to be done by the procedure mentioned in Appendix-F. The torque applied to the output-link as a function of crank angle is shown in Figure 4.10:

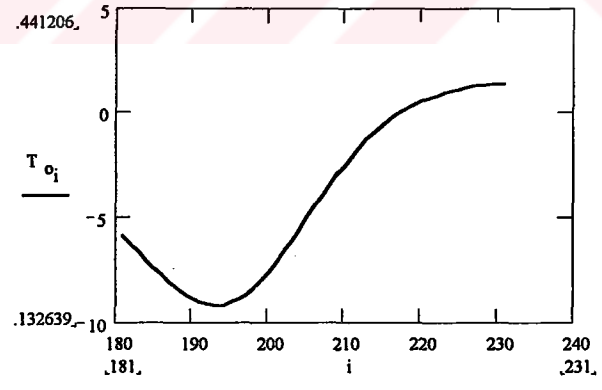

Figure 4.10: Torque applied to the Output-Link

In Figure 4.9, the graph on the left side is the position and the graph on the right side is the velocity, acceleration (dashed line) of the control-link. At the end of

the switching (when crank angle is 231^0), it is seen that $\zeta = \alpha = -18{,}3$ which is the same with obtained from the synthesis procedure. (In addition, there is no discontinuity in the curve, which is a necessary condition for movability of the mechanism.

According to Figure 4.10, the torque applied to the output-link link has a peak value of 9.13 N.m. in clockwise direction. The output-link can move only in clock-wise direction when at least 10 N.m. is applied. Then, it is proved that the output-link remains also steady during switching to second position. Therefore, switching first to second position is possible under the conditions assumed in Example 5.

Similarly, using the same procedure, the output-link torque for switching second to first positions is determined and shown in Figure 4.11.

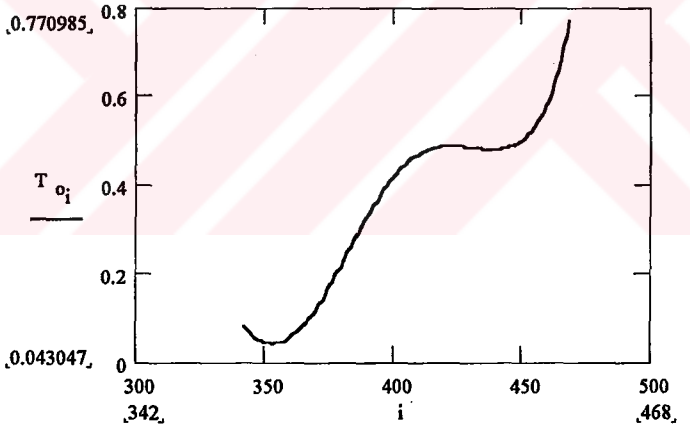

Figure 4.11 Torque applied to the Output-Link at the Second Position

During switching second to first positions, the output-link can only move in counter clockwise direction. In addition, in order to overcome the friction force on the output-link, at least 2 N.m. torque (CCW) must be applied to the output-link. According to Figure 4.10, since the maximum value of the torque applied to the output-link is +0.8 N.m., the output-link remains stationary and so switching second to first position is also possible.

CHAPTER 5

DISCUSSION and CONCLUSION

5.1 Discussion

During the kinematic synthesis of the first type of variable structure mechanism (Figure 3.1), three free parameters are obtained. These are; initial stroke position (s_{e1}), initial output-link angle (θ_{e1}) of the second slider crank mechanism and parameter p which is the unique parameter that determines the link-proportions of the first slider-crank. After optimization, it is seen that variation of p has a very slight effect on the transmission angle and on the link proportions of second slider. Therefore, this parameter is kept constant (a suitable value is chosen for an acceptable transmission angle deviation for the first slider-crank) during optimization. The other two free parameters have a nearly linear relation with the optimization objectives. Therefore, by trial-error for the required output-link oscillations acceptable solutions are obtained easily.

Switching, which is the motion of the control-link in between specified positions, is to be performed due to the variation of the output-link torque without an external control. If there is a sudden increase in the output-link torque during forward stroke, the mechanism will switch to other position (smaller output-link oscillation position).

Moreover, when the output-link torque decreases to a specific value the mechanism will switch back to its first position. This phenomenon is called as "Automatic Switching". In application, this type of switching is a required case.

However, after the low-speed switching analysis, it is seen that it is not possible to obtain such kind of mechanism that automatically switches. In order to overcome the switching problems, two simple modifications are applied to the mechanism (shown in part 4.2.2-3), which makes automatic switching possible in certain cases. In application, to obtain a reliable system, the parts used in modification procedure must be carefully manufactured. Now, another alternative for switching, using an electrical switch at the control-link, which is controlled externally, comes into consideration, as the modification procedure becomes complicated. Because at the beginning of the study, the objective is to obtain a low-cost and simple mechanism that can switch automatically and it is not clear to obtain such a mechanism with the modifications mentioned. Therefore, according to cost and reliability a careful comparison must be done between modifications and external control.

In the high-speed switching analysis, in order not to come across with the same problems an external control attached to the control-link is assumed. Switching is performed at the extreme positions of the mechanism where the output-link remains steady at both instant of start and during switching. In theory, a model can be synthesized that has a moving output-link during switching. However, the author believes that for this case, due to manufacturing and the working conditions imperfections a real model may not work as desired or the mechanism may lock during switching.

5.2 Conclusion

In this study, a design procedure for two different types of two degree-of-freedom mechanisms is accomplished. The variable structure mechanism performs different oscillations at the output-link.

Kinematic and force analysis of the mechanisms that synthesized is done for both low-speed and high-speed operations (where inertia forces are also regarded). According to the control-link torque, with a switch element, the motion of the control-link (second input) is investigated to obtain different oscillation at the output.

The kinematic synthesis technique, mentioned in this study, can be applied to other type of two degree-of-freedom mechanisms easily.

A model can be built to see whether switching of the control-link due to the variation of the output-link torque is possible or not.

APPENDICES

Appendix-A: Position Analysis of the Seven-Link Mechanism

Angular position of the output-link will be determined as a function of crank position or the input. Also, the angles, which are needed for the force analysis, will be determined.

Initially, the relation between crank angle and stroke will be determined for both slider-cranks:

Since the first slider-crank is an in-line type, the relation between crank angle ϕ and stroke s_1 can be easily found by applying cosine law:

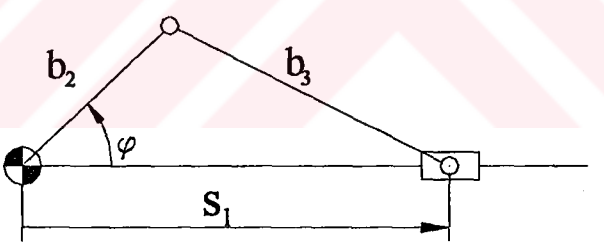

Figure A.1: First Slider-Crank

$$b_3^2 = b_2^2 + s_1^2 - 2 \cdot b_2 \cdot s_1 \cdot \cos\phi$$

Or,

$$s_1 = b_2 \cdot \cos\phi \pm \sqrt{b_3^2 - b_2^2 \cdot \sin^2\phi}\,. \qquad \text{(A.1)}$$

Where plus or minus sign refers to two different configurations. According to the configuration used in Figure A.1 s_1 is positive for all crank angles ($b_3 > b_2$) so Equation (A.11) becomes:

$$s_1 = b_2 \cdot \cos\phi + \sqrt{b_3^2 - b_2^2 \cdot \sin^2\phi} \qquad \text{(A.2)}$$

For the second slider-crank the relations between slider position s_2, output-link angle θ and β at the first position are:

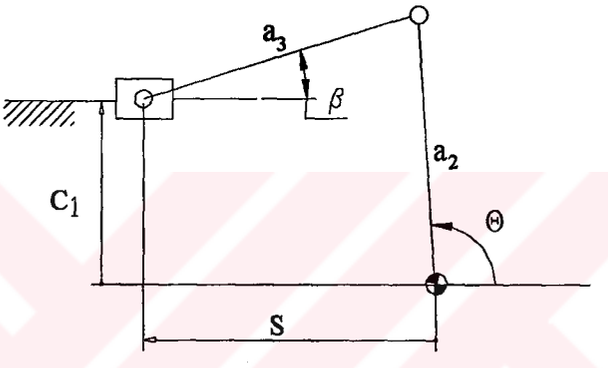

Figure A.2: Second Slider-Crank

$$a_3 \cdot \cos\beta = s_2 + a_2 \cdot \cos\theta,$$

$$a_3 \cdot \sin\beta = a_2 \cdot \sin\theta - c_1.$$

Squaring and adding these equations side by side, angle β will be eliminated and Equation (A.3) is obtained:

$$s_2 \cdot \cos\theta - c_1 \cdot \sin\theta = \frac{a_3^2 - a_2^2 - s_2^2 - c_1^2}{2 \cdot a_2} \qquad \text{(A.3)}$$

Substituting the below trigonometric identities into Equation (A.3),

$$\sin\theta = \frac{2\cdot\tan\left(\frac{1}{2}\theta\right)}{1+\tan^2\left(\frac{1}{2}\theta\right)}$$

$$\cos\theta = \frac{1-\tan^2\left(\frac{1}{2}\theta\right)}{1+\tan^2\left(\frac{1}{2}\theta\right)}$$

A quadratic in terms of $\tan(\theta/2)$ can be obtained and the solution of this equation is:

$$\theta = 2\cdot\tan^{-1}\left(\frac{-c_1 \pm \sqrt{c_1^2+s_2^2-m^2}}{m+s_2}\right) \qquad \text{(A.4)}$$

Where m is,

$$m = \frac{a_3^2 - a_2^2 - s_2^2 - c_1^2}{2\cdot a_2}$$

Since $s_1 + s_2$ is constant for all positions of the slider, s_2 can be easily found in terms of the constants and s_1 from the Figure A.3:

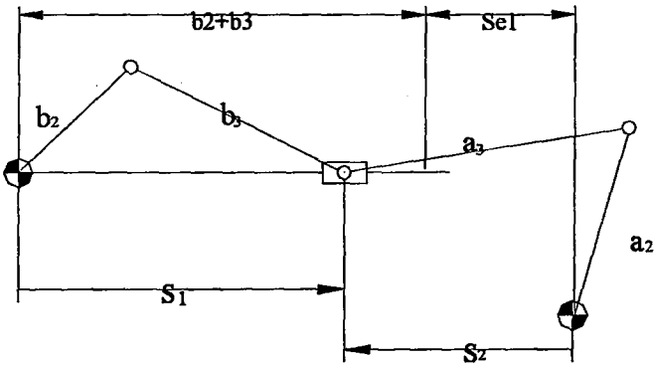

Figure A.3: Stroke Relations at the First position

$$s_1 + s_2 = b_2 + b_3 + s_{e1},$$

Or,

$$s_2 = b_2 + b_3 + s_{e1} - s_1 \tag{A.5}$$

Substituting s_1 in Equation (A.5) into Equation (A.2), s_2 can be obtained as a function crank angle position ϕ:

$$s_2 = b_2 + b_3 + s_{e1} - b_2 \cdot \cos\phi - \sqrt{b_3^2 - b_2^2 \cdot \sin^2\phi} \tag{A.6}$$

Also, if s_2 is substituted into Equation (A.4), output-link angle θ can be obtained as a function of crank angle ϕ.

After switching since the geometry of the mechanism changes, Equations (A.1-6) are valid for only first position of the variable structure mechanism. So, these equations must be modified according to second position.

After switching Equation (A-2) becomes:

$$s_1 = b_2 \cdot \cos(\phi + \alpha) + \sqrt{b_3^2 - b_2^2 \cdot \sin^2(\phi + \alpha)} \tag{A.7}$$

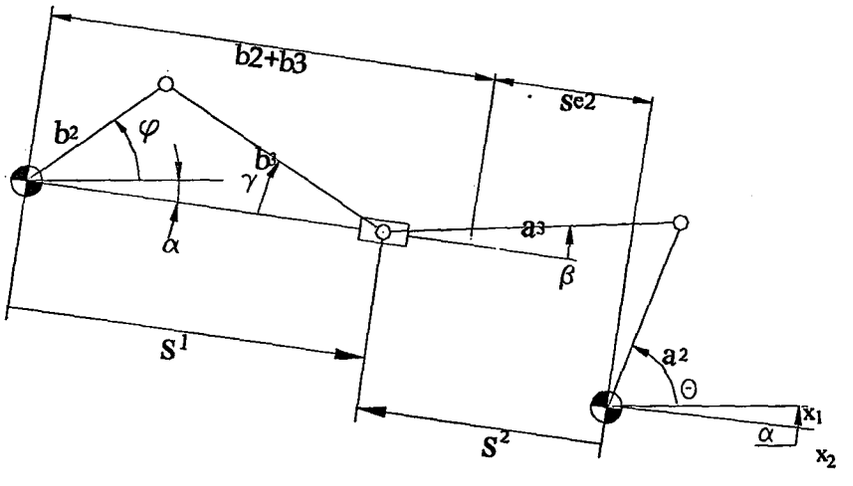

Figure A.4: Stroke Relations at the Second Position

And Equation (A.5) becomes:

$$s_2 = b_2 + b_3 + s_{e1} - s_1 \tag{A.8}$$

Substituting (A.7) into Equation (A.8):

$$s_2 = b_2 + b_3 + s_{e2} - b_2 \cdot \cos(\phi + \alpha) - \sqrt{b_3^2 - b_2^2 \cdot \sin^2(\phi + \alpha)} \tag{A.9}$$

Also Equation (A.3) becomes:

$$s_2 \cdot \cos(\theta + \alpha) - c_2 \cdot \sin(\theta + \alpha) = \frac{a_3^2 - a_2^2 - s_2^2 - c_2^2}{2 \cdot a_2} \tag{A.10}$$

By using the same procedure for simplifying Eqn (A.3) to Eqn (A.4), Eqn (A.10) becomes:

$$\theta = 2 \cdot \tan^{-1}\left(\frac{-c_2 \pm \sqrt{c_2^2 + s_2^2 - m^2}}{m + s_2}\right) - \alpha \tag{A.11}$$

Where m is,

$$m = \frac{a_3^2 - a_2^2 - s_2^2 - c_2^2}{2 \cdot a_2}$$

The two angles γ and β (Figure A.4) which are also needed for the force analysis must be determined in an appropriate form.

Angle γ can be obtained in terms of the crank angle, by applying sine law to first slider crank (Figure A.5) as:

$$\gamma = a\sin\left[\frac{b_2}{b_3}\cdot\sin(\phi+\alpha)\right], \tag{A.12}$$

where α is zero in the first position.

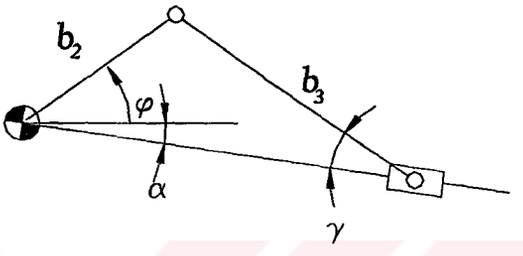

Figure A.5 :First Slider-Crank

β can be obtained with a similiar method used to derive Eqn (A.4) as:

$$\beta = 2\cdot\tan^{-1}\left(\frac{c_1 \pm \sqrt{c_1^2 + s_2^2 - m^2}}{m - s_2}\right) \tag{A.13}$$

Where m is:

$$m = \frac{a_2^2 - a_3^2 - s_2^2 - c_1^2}{2\cdot a_3} \tag{A.14}$$

β in the second position can be obtained by replacing c_1 with c_2 in Equations (A.13) and (A.14).

Appendix-B: Static Force Analysis of the Mechanism

In this part, the torque applied to the control link from the slider due to required output-link torque will be calculated. During the static force analysis, friction forces will be neglected.

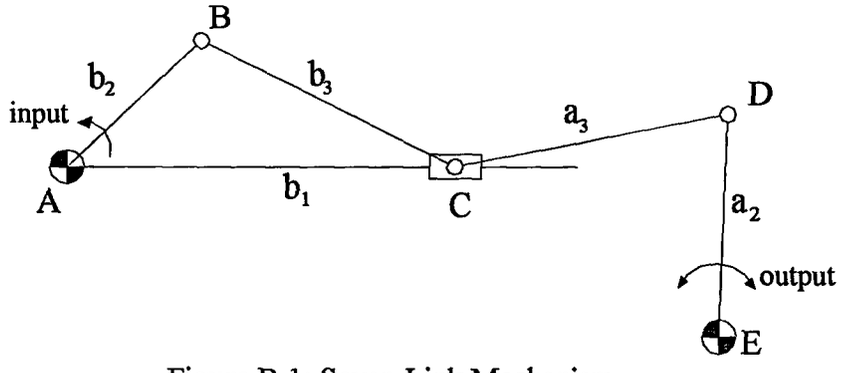

Figure B.1: Seven-Link Mechanism

By taking moment about E, the force applied from link a_3 to a_2 can be calculated as:

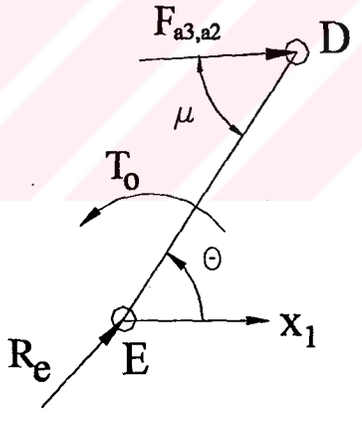

Figure B.2: Free body diagram of Link a_2

$$\Sigma M_E = 0 \ \text{(CCW +)},$$

$$T_o - a_2 \cdot F_{a3,a2} \cdot \sin\mu = 0,$$

$$F_{a3,a2} = \frac{T_o}{a_2 \cdot \sin \mu}. \qquad \text{(B.1)}$$

Since link a_3 is a two-force member:

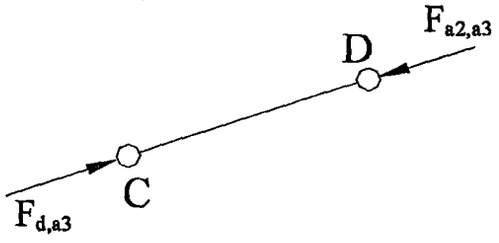

Figure B.3 : Free Body Diagram of Link a_3

$$F_{d,a3} = -F_{a2,a3} = F_{a3,a2} \qquad \text{(B.2)}$$

From the free body diagram of the slider's pin, by using moving *n-t* coordinate (*t* is collinear with the slider axis at all positions), the normal force acting on the slider is (Figure B.4):

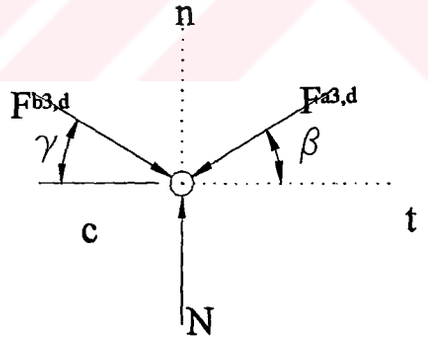

Figure B.4: Free Body Diagram of the Slider's Pin

$$\Sigma F_t = 0,$$

$$F_{b3,d} \cdot \cos\gamma - F_{a3,d} \cdot \cos\beta = 0, \qquad \text{(B.3)}$$

$$\Sigma F_n = 0,$$

$$-F_{b3,d} \cdot \sin\gamma - F_{a3,d} \cdot \sin\beta + N = 0, \qquad \text{(B.4)}$$

Eleminating $F_{b3,d}$ from Eqn. (B.4) by Eqn. (B.3),

$$N = F_{a3d} \cdot \sin\beta + \sin\gamma \cdot F_{a3d} \cdot \frac{\cos\beta}{\cos\gamma}. \qquad \text{(B.5)}$$

Since $F_{a3,d} = F_{a3,a2}$ (B.2),

$$N = F_{a3,a2} \cdot (\sin\beta + \tan\gamma \cdot \cos\beta). \qquad \text{(B.6)}$$

And by using Equation (B.1) N can be re-written as:

$$N = \frac{T_o \cdot (\sin\beta + \tan\gamma \cdot \cos\beta)}{a_2 \cdot \sin\mu}. \qquad \text{(B.7)}$$

The resultant torque applied on the control-link by the slider is (Figure B.5):

$$T_c = -s_1 \cdot N \qquad \text{(B.8)}$$

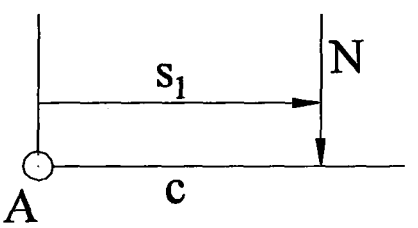

Figure B.5: Normal Force on the Control Link

There is a minus sign in Equation (B.8), because according to Figure, if N is positive, the torque applied on the control link must be negative (CCW +).

Subsituting N from Eqn. (B.7) into Eqn (B.8), the torque applied on the control-link can be obtained as a function of the output-link as:

$$T_c = -s_1 \cdot \frac{T_o \cdot (\sin\beta + \tan\gamma \cdot \cos\beta)}{a_2 \cdot \sin\mu} \tag{B.9}$$

Equation (B.9) is valid for both positions of the mechanism. But note that, stroke s_1 and the angles in the Equation are also function of the control-link's position and these position parameters are clearly defined in Appendix-A.

Appendix-C: Velocity and Acceleration Analysis of the Seven-Link Mechanism

Determining only the acceleration of the slider and link a_2 will be enough to investigate the torque applied to the control-link from the slider. Note that, crank speed is assumed constant.

The analysis will be done at second position of the mechanism. By taking switching angle α as zero the equations will also be valid at the first position of the mechanism.

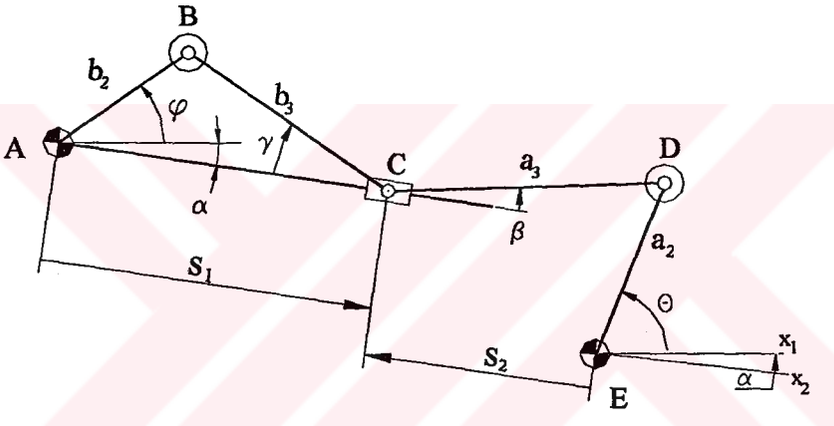

Figure C.1: Seven-Link Mechanism at Second Position

The slider position as a function of crank angle can be determined as:

$$\begin{aligned} s_1 &= b_2\cos(\phi+\alpha)+b_3\cos(\gamma+\alpha) \\ &= b_2\cos(\phi+\alpha)+b_3\sqrt{1-((b_2/b_3)\cdot\sin(\phi+\alpha))^2} \end{aligned} \qquad \text{(C.1)}$$

If the second term is expanded by using binomial theorem and neglecting all but the first two terms, Equation (C.2) can be obtained:

$$s_1 = b_2\cos(\varphi+\alpha)+b_3\left(1-\frac{b_2^2}{2b_3^2}\sin^2(\varphi+\alpha)\right),$$

Or,

$$s_1 = b_3 - \frac{b^2}{4b_3} + b_2(\cos(\phi+\alpha) + \frac{b_2}{4b_3}\cos 2(\phi+\alpha)). \quad \text{(C.2)}$$

By derivation of Eqn. (C.2) with respect to time, velocity and acceleration can be obtained for constant crank speed ϕ_d as:

$$\dot{s}_1 = -\phi_d \cdot b_2 \cdot (\sin(\phi+\alpha) + \frac{b_2}{2b_3}\sin 2(\phi+\alpha)) \quad \text{(C.3)}$$

$$\ddot{s}_1 = -\phi_d^2 \cdot b_2 \cdot (\cos(\phi+\alpha) + \frac{b_2}{b_3}\cos 2(\phi+\alpha)) \quad \text{(C.4)}$$

According to Figure 44 $\dot{s}_2 = -\dot{s}_1$ and $\ddot{s}_2 = -\ddot{s}_1$.

By derivation of Eqn. (A.10), angular velocity and acceleration of the output-link can be obtained as:

$$\dot{\theta} = \frac{(\cos(\theta+\alpha) + \frac{s_2}{a_2}) \cdot \dot{s}_2}{s_2 \sin(\theta+\alpha) + c_2 \cos(\theta+\alpha)} \quad \text{(C.5)}$$

$$\ddot{\theta} = \frac{\ddot{s}_2(s_2/a_2) + (\dot{s}_2^2/a_2) + (\ddot{s}_2 - s_2\dot{\theta}^2)\cos(\theta+\alpha) + (\dot{\theta}^2 c_2 - 2\dot{s}\dot{\theta})\sin(\theta+\alpha)}{s_2 \sin(\theta+\alpha) + c_2 \cos(\theta+\alpha)} \quad \text{(C.6)}$$

Where s_2 can be calculated from Eqn. (A.9) and θ can be calculated from Equation (A.11).

In Equations (C.1-6), if switching angle α is taken as zero and eccentricity of the second slider-crank at second position c_2 is replaced with c_1, the output-link angle and the slider acceleration can be calculated from (C.4) and (C.6) for first the position.

Appendix-D: Dynamic Force Analysis of the Seven-Link Mechanism

According to Figure (25), the connecting rod b_3 and a_3 can be divided into two concentrated mass type links. As an example, mass distribution of the link b_3 is done according to relations below:

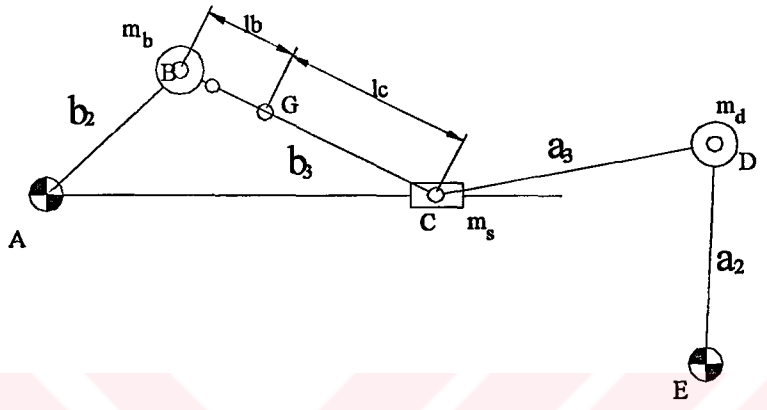

Figure D.1: Variable Structure Mechanism with Concentrated Masses

$$m_{b3} = m_{b3B} + m_{b2C}, \tag{D.1}$$

$$m_{b3B} \cdot l_{Bb} = m_{b3C} \cdot l_C, \tag{D.2}$$

$$I_G = m_{b3B} \cdot l_b^2 + m_{b3C} \cdot l_C^2. \tag{D.3}$$

Equation (D.1), (D.2) and (D.3) must be satisfied simultaneously to obtain exact dynamic equivalent system. But with two free parameters (m_{b3B} and m_{b3A}), three equations can't be satisfied. In usual connecting rods, the center of gravity is close to crankpin (due to internal stresses). And when (D.1) and (D.2) are solved together to obtain portions of the concentrated masses on each side, it is seen that Equation (D.3), the moment of inertia of the rod, is also satisfied with an acceptable error. The simultaneous solution of (D.1) and (D.2) yields:

$$m_{b3B} = m_{b3} \cdot \frac{l_c}{lc + l_b} \tag{D.4}$$

$$m_{b3C} = m_{b3} \cdot \frac{l_b}{lc + l_b} \tag{D.5}$$

Since input crank angle is assumed to rotate at a constant rate, amount of concentrated mass at B becomes unimportant in determining the control-link torque.

According to the free body diagram of the output-link a_2, F_D can be calculated by taking moment about E ($\sum M_E = I_{a_2} \cdot \ddot{\theta}$, as CCW +). The direction of the force F_D is along the link a_3, since this link becomes a two-force member after concentrated mass approach:

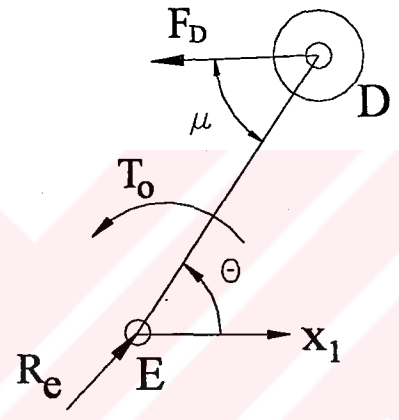

Figure D.2: Free Body Diagram of Link a_2

$$T_o + a_2 \cdot F_D \cdot \sin\mu = I_{a2} \cdot \ddot{\theta},$$

Or,

$$F_D = \frac{I_{a2} \cdot \ddot{\theta} - T_o}{a_2 \cdot \sin\mu}. \tag{D.6}$$

Where mass moment of inertia of the link a_2 about E is:

$$I_{a2} = m_d \cdot a_2^2$$

According to the free body diagram of the slider in Figure D.3, the sum of the forces acting to the slider will be equal to the concentrated mass portion at slider multiplied by slider acceleration:

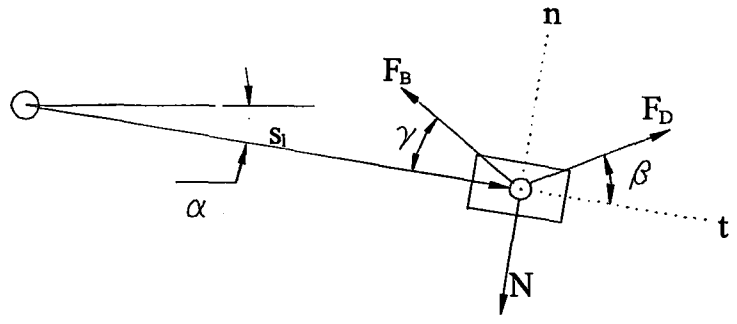

Figure D.3: Free Body Diagram of the Slider

Note that, forces F_B and F_D are also two-force members and they act along links b_3 and a_3 respectively (Figure D.1).

$$\sum F_t = m_s \cdot \ddot{s}_1$$

$$F_B \cdot \cos\gamma - F_D \cdot \cos\beta = -\ddot{s}_1 \cdot m_s$$

Or,

$$F_B = \frac{F_D \cdot \cos\beta - \ddot{s}_1 \cdot m_s}{\cos\gamma} \qquad \text{(D.7)}$$

And since there is no motion in n-direction, there is a static equilibrium in this direction:

$$\sum F_n = 0$$

$$N = F_B \cdot \sin\gamma + F_D \cdot \sin\beta \qquad \text{(D.8)}$$

The torque acting on the control-link from the slider is:

$$T_c = s_1 \cdot N \tag{D.9}$$

From Equations (D.7)-(D.9) the torque applied to the control-link can be found as a function of external torque applied to the output-link as:

$$T_c = s_1 \cdot \left(\frac{I_{a2}\ddot{\theta} - T_o}{a_2 \sin\mu}\right) \cdot (\cos\beta \tan\gamma + \sin\beta) - s_1 \cdot \ddot{s}_1 m_s \tan\gamma \tag{D.10}$$

The position parameters in Eqn. (D.10) are given according to crank position in Appendix-A for both positions of the mechanism. Acceleration of the output-link angle and the slider are given in Appendix-C.

Appendix-E: Kinematic Analysis of the Mechanism during Switching

The parameters ζ, η, ψ and s shown in Figure E.1 must be determined as a function of crank angle.

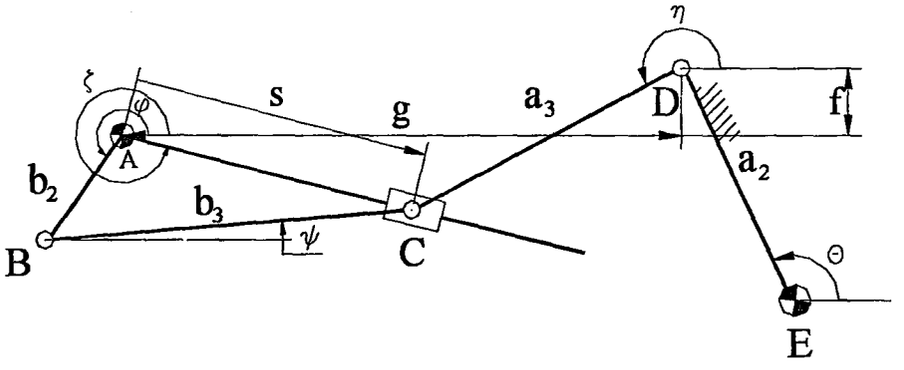

Figure E.1: Six-link Mechanism Obtained during Switching

In order to determine angle η as a function of input φ, loop closure equation (E.1) and its complex conjugate (E.2) can be written (**BC = -AB + g + f + DC**):

$$b_3 e^{i\psi} = -b_2 e^{i\varphi} + g + if + a_3 e^{i\eta} \qquad \text{(E.1)}$$

$$b_3 e^{-i\psi} = -b_2 e^{-i\varphi} + g - if + a_3 e^{-i\eta} \qquad \text{(E.2)}$$

Where:

$$f = c_1 - a_2 \cos\theta,$$

$$g = b_2 + b_3 + s_{e1} + a_2 \cos\theta.$$

Note that f and g remain constant during switching.

To eliminate ψ Equations (E.1) and (E.2) can be multiplied side by side:

$$b_3^2 = (-b_2 e^{i\varphi} + g + if + a_3 e^{i\eta}) \cdot (-b_2 e^{-i\varphi} + g - if + a_3 e^{-i\eta}) \qquad \text{(E.3)}$$

After manipulating Equation (E.3), the angle η can be obtained as a function of φ in closed-form:

$$\eta = 2\arctan\left[\frac{B \pm \sqrt{B^2 + A^2 - C^2}}{A + C}\right] \tag{E.4}$$

Where:

$$A = g - b_2 \cos\varphi, \quad B = f - b_2 \sin\varphi,$$

$$C = \frac{b_3^2 - b_2^2 - g^2 - f^2 - a_3^2}{2a_3} + \frac{b_2}{a_3}(f \sin\varphi + g\cos\varphi).$$

According to Figure E.1, second loop closure eqaution can be written from **AC = g + if + DC:**

$$s \cdot e^{i\zeta} = g + if + a_3^{i\eta} \tag{E.5}$$

Now since η is known, s and ζ can be easily calculated from Eqn. (E.5):

$$s = \left|g + if + a_3 e^{i\eta}\right| \tag{E.6}$$

$$\zeta = \angle(g + if + a_3 e^{i\eta}) \tag{E.7}$$

And ψ can be determined from Equation (E.1) as:

$$\psi = \angle(g + if + a_3 e^{i\eta} - b_2 e^{i\varphi}) \tag{E.8}$$

The velocity of the links can be determined for constant crank speed (φ_d), by derivation of Equations (E.1), (E.5) and their complex conjugates with respect to time.

Manipulating the derived equations, Eqn. (E.9) can be obtained as:

$$A \cdot B = C$$

Or,

$$B = A^{-1} \cdot C \tag{E.9}$$

Where:

$$A = \begin{bmatrix} j \cdot b_3 \cdot e^{j\cdot\psi} & -j \cdot a_3 \cdot e^{j\cdot\eta} & 0 & 0 \\ -j \cdot b_3 \cdot e^{-j\cdot\psi} & j \cdot a_3 \cdot e^{-j\cdot\eta} & 0 & 0 \\ 0 & -j \cdot a_3 \cdot e^{j\cdot\eta} & j \cdot s \cdot e^{j\cdot\zeta} & e^{j\cdot\zeta} \\ 0 & j \cdot a_3 \cdot e^{-j\cdot\eta} & -j \cdot s \cdot e^{-j\cdot\zeta} & e^{-j\cdot\zeta} \end{bmatrix} \quad B = \begin{bmatrix} \psi_d \\ \eta_d \\ \zeta_d \\ s_d \end{bmatrix}$$

$$C = \phi_d \cdot \begin{bmatrix} -j \cdot b_2 \cdot e^{j\cdot\phi} \\ j \cdot b_2 \cdot e^{-j\cdot\phi} \\ 0 \\ 0 \end{bmatrix}$$

Note that, A is the coefficient matrix involving position variables, B is the column vector whose components are the rate change of position variables, C is the column vector involving position variables and input velocity.

Similarly, acceleration of the links can be determined for constant crank speed (φ_d), by second derivative of Equations (E.1), (E.5) and their complex conjugates with respect to time.

Manipulating the derived Equations, (E.10) can be obtained:

$$A \cdot E = D$$

Or,

$$E = A^{-1} \cdot D \tag{E.9}$$

$$D = \begin{bmatrix} -a_3 \cdot \eta \, d^2 \cdot e^{j \cdot \eta} + b_3 \cdot \psi \, d^2 \cdot e^{j \cdot \psi} + b_2 \cdot \phi \, d^2 \cdot e^{j \cdot \phi} \\ -a_3 \cdot \eta \, d^2 \cdot e^{-j \cdot \eta} + b_3 \cdot \psi \, d^2 \cdot e^{-j \cdot \psi} + b_2 \cdot \phi \, d^2 \cdot e^{-j \cdot \phi} \\ -2 \cdot j \cdot s \, d \cdot \zeta \, d \cdot e^{j \cdot \zeta} + \zeta \, d^2 \cdot s \cdot e^{j \cdot \zeta} - a_3 \cdot \eta \, d^2 \cdot e^{j \cdot \eta} \\ 2 \cdot s \, d \cdot j \cdot \zeta \, d \cdot e^{-j \cdot \zeta} + \zeta \, d^2 \cdot s \cdot e^{-j \cdot \zeta} - a_3 \cdot \eta \, d^2 \cdot e^{-j \cdot \eta} \end{bmatrix} \qquad E = \begin{bmatrix} \psi \, dd \\ \eta \, dd \\ \zeta \, dd \\ s \, dd \end{bmatrix}$$

From Equation (E.10), acceleration of each link can be determined.

Appendix-F: Force Analysis of the Mechanism during Switching

Initially, necessary free-body diagrams of the links diagrams must be drawn. The control-link's free body diagram is shown in Figure F.1.

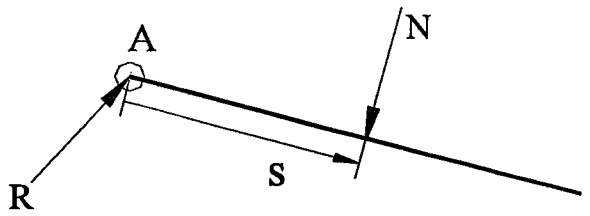

Figure F.1: Free Body Diagram of the Control-Link

Since the control-link has a motion of fixed axis rotation about A, one may take moment around A and obtain N as (During the force analysis CCW will be taken as positive direction):

$$\sum M_A = I_{cA}\alpha,$$

$$N = \frac{-I_{cA}\cdot\ddot{\zeta}}{s} \qquad \text{(F.1)}$$

Where:

$$I_{cA} = \frac{1}{3}m\cdot l_c^{\,2}$$

In Figure F.2, free-body diagram of the slider is shown. Due to the concentrated mass approach, link a_3 and b_3 become two-force member so the forces acting to these links are along the direction of the link.

The moving *n-t* coordinate in Figure F.2 is assumed to be attached to link a_3

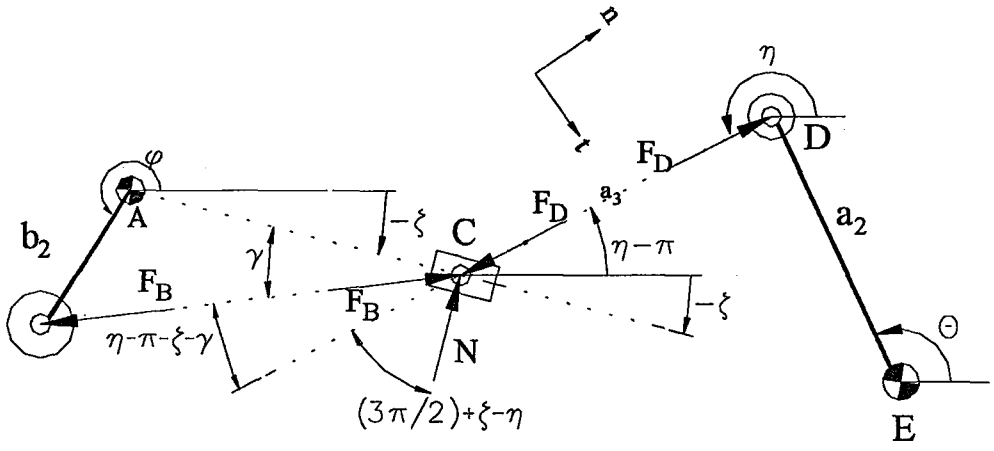

Figure F.2: Free Body Diagram of the Slider

According to Figure F.2:

$$\sum F_n = m_C (a_C)_n$$

$$N\cos(\frac{3}{2}\pi + \zeta - \eta) + F_B \cos(\eta - \pi - \zeta - \gamma) - F_D = m_C (a_C)_n \qquad \text{(F.2)}$$

And,

$$\sum F_t = m_C (a_C)_t$$

$$-N\sin(\frac{3}{2}\pi + \zeta - \eta) + F_B \sin(\eta - \pi - \zeta - \gamma) = m_C (a_C)_t \qquad \text{(F.3)}$$

Where:

$$(a_C)_n = a_3 \cdot \dot{\eta}^2$$
$$(a_C)_t = a_3 \cdot \ddot{\eta}$$

The force acting to output-link, F_D, can be determined by eliminating F_B from Equations (F.2) and (F.3):

$$F_D = N\sin(\zeta-\eta)-(N\cos(\zeta-\eta)-m_c(a_c)_t)\cot(\eta-\zeta-\gamma)-m_c(a_c)_t \quad \text{(F.4)}$$

And from Figure F.2 the torque applied to the output-link during switching can be determined as:

$$T_o = -a_2 F_D \sin(\eta-\theta) \quad \text{(F.5)}$$

REFERENCES

[1] T. S. Mruthunjaya, "A Note on Synthesis of the General, Two-Degree-of-Freedom Linkage", Mechanism and Machine Theory, Vol. 10, p. 77-80, 1975.

[2] V. Handra - Luca, "The Study of Adjustable Oscillating Mechanisms", J. Engng. md. Trans. ASME, p. 677-680, August 1973.

[3] D. Kohli - A. H. Soni, "Synthesis of Seven-Link Mechanisms", J. Engng. md. Trans. ASME, p. *533-540,* May 1973

[4] A. Ahmad - K. J. Waldron, "Synthesis of Adjustable Planar 4-bar Mechanisms", Mechanism and Machine Theory, Vol. 14, p. 405-411, July 1979.

[5] T. Chuenchom – S. Kota, "Synthesis of Programmable Mechanisms Using Adjustable Dyads", Journal of Mechanical Design, Vol. 119, June 1997

[6] A. Akmeşe – E. Söylemez, " Two Degrees of Freedom Adjustable Mechanisms Design"

[7] A. Kireçci - L. C. Dulger - H. M. Gultekin, "Design of Hybrid Actuator", 8~ international Machine Design and Production Conference Proceedings, p. 65-74, September 1998.

[8] F. Freudenstein- E. Söylemez, " The Multiport Lever: A Mechanical Logic Element", J. Engng Ind., p. 353-359, May 1977.